



# Life cycle cost assessment of railways infrastructure asset under climate change impacts

Khosro Soleimani-Chamkhorami<sup>a,d,\*</sup>, A.H.S Garmabaki<sup>a</sup>, Ahmad Kasraei<sup>a</sup>,  
Stephen M. Famurewa<sup>a,b</sup>, Johan Odelius<sup>a</sup>, Gustav Strandberg<sup>c</sup>

<sup>a</sup> Department of Civil, Environmental, and Natural Resources Engineering, Division of Operation and Maintenance, Luleå University of Technology,

SE-97187 Luleå, Sweden

<sup>b</sup> Swedish Transport Administration, Luleå, Sweden

<sup>c</sup> Rossby Centre, Swedish Meteorological and Hydrological Institute, SMHI, Sweden

<sup>d</sup> Department of Mathematics, Faculty of Computer Engineering, Najafabad Branch, Islamic Azad University, Najafabad, Iran

## ARTICLE INFO

### Keywords:

Climate adaptation  
Climate change  
Life cycle cost analysis  
Proportional hazard model  
Railway infrastructure  
Reliability analysis

## ABSTRACT

Climate change impacts such as extreme temperatures, snow and ice, flooding, and sea level rise posed significant threats to railway infrastructure networks. One of the important questions that infrastructure managers need to answer is, “How will maintenance costs be affected due to climate change in different climate change scenarios?” This paper proposes an approach to estimate the implication of climate change on the life cycle cost (LCC) of railways infrastructure assets. The proportional hazard model is employed to capture the dynamic effects of climate change on reliability parameters and LCC of railway assets. A use-case from a railway in North Sweden is analyzed to validate the proposed process using data collected over 18 years. The results have shown that precipitation, temperature, and humidity are significant weather factors in selected use-case. Furthermore, our analyses show that LCC under future climate scenarios will be about 11 % higher than LCC without climate impacts.

## 1. Introduction

Climate change and its consequences, such as the increased intensity and frequency of extreme weather events, pose significant challenges to the efficiency of railway network operations and associated costs. In northern Europe, harsh weather phenomena, including heavy rain, snowfall, freezing temperatures, and strong winds, have the potential to disrupt and impair railway infrastructure. Research indicates that adverse climatic conditions account for 5 to 10 % of overall system failures, contributing to 60 % of delays in this particular railway network region (Garmabaki et al., (2021) and Thaduri et al., (2021)). The considerable uncertainty in adaptation to climate change risks presents a profound challenge for planners and decision-makers (Wang et al., (2020) and Blackwood and Renaud, (2022)). Some studies have been conducted to assess the impact of climate change on transportation infrastructure and the associated costs. For instance, Swarna et al., (2022) evaluated the Global Warming Potential (GWP) on life cycle assessment (LCA)

\* Corresponding author at: Division of Operation and Maintenance, Department of Civil, Environmental, and Natural Resources Engineering, Luleå University of Technology, SE-97187 Luleå, Sweden.

E-mail addresses: [khosro.soleimani.chamkhorami@associated.ltu.se](mailto:khosro.soleimani.chamkhorami@associated.ltu.se) (K. Soleimani-Chamkhorami), [Amir.garmabaki@ltu.se](mailto:Amir.garmabaki@ltu.se) (A.H.S Garmabaki), [Ahmad.kasraei@associated.ltu.se](mailto:Ahmad.kasraei@associated.ltu.se) (A. Kasraei), [stephen.famurewa@trafikverket.se](mailto:stephen.famurewa@trafikverket.se) (S.M. Famurewa), [johan.odelius@ltu.se](mailto:johan.odelius@ltu.se) (J. Odelius), [Gustav.Strandberg@smhi.se](mailto:Gustav.Strandberg@smhi.se) (G. Strandberg).

<https://doi.org/10.1016/j.trd.2024.104072>

Received 18 September 2023; Received in revised form 12 December 2023; Accepted 10 January 2024

Available online 19 January 2024

1361-9209/© 2024 The Author(s). Published by Elsevier Ltd. This is an open access article under the CC BY license (<http://creativecommons.org/licenses/by/4.0/>).

and life cycle cost analysis/assessment (LCCA) for climate change adaptation options in various Canadian locations. [Liu, K. et al., \(2021\)](#) calculated the risk faced by Chinese railway infrastructure under different periods and warming levels in combination with climate models. Their analysis shows that by keeping warming to 1.5 °C instead of 3 °C, the Chinese railway can save 2.06 billion/year. [Banar and Özdemir, \(2015\)](#) evaluated Turkey's railway passenger transportation system from an environmental and economic aspect using LCA and LCC methodologies. Their findings indicate that 58 % of the total environmental impact of high-speed railways comes from infrastructure and 42 % from operations. Conversely, for conventional railways, the infrastructure accounts for 39 % of the environmental burden, while operations contribute 61 %. [Pu et al., \(2023\)](#) formulated a carbon emissions model for railway alignment optimization involving three stages: construction, operation, and maintenance during a railway's life cycle. The proposed model is combined with a cost function to create a bi-objective model and solved with a particle swarm algorithm. Their results analysis shows that cost-emission balanced alignment is 8.0 % cheaper than manually designed alignment and reduces life-cycle carbon emissions by 4.2 % compared to manually designed alignment.

The research by [Chinowsky et al., \(2019\)](#), utilizing various climate models, suggests that the US rail network could experience a rise in delay-minute expenses. Historically, these costs could increase from \$25 to \$45 billion cumulatively by 2100 in a scenario with low greenhouse gas emissions. These expenses could escalate between \$35 to \$60 billion in a high-emission scenario. In addition, [Cahyo et al., \(2021\)](#) investigated the impact of climate change on the operation of the US rail network, highlighting the potential sensitivity of this system to projected temperature rises. In another study, [Garmabaki et al., \(2021\)](#) offered recommendations to enhance climate resilience in transportation networks by assessing vulnerabilities and utilizing climate adaptation measures and actions on railway infrastructure. [Hamarat et al., \(2019\)](#) carried out LCC analysis of railway assets exposed to climate change. They indicate that crossing renewal, tamping activities, and miscellaneous maintenance bear high costs. [Piryonesi and El-Diraby, \(2021\)](#) investigate the impact of climate change on road infrastructure using a machine learning approach for predicting pavement condition index. [Neumann et al., \(2021\)](#) estimated the impacts of climate change on railroads, roads, and coastal properties under three infrastructure management response scenarios, including no adaptation, reactive adaptation, and proactive adaptation. They indicated proactive actions reduce total costs across all three sectors to the low \$10 s of billions annually. [Qiao et al., \(2022\)](#) introduced a comprehensive methodological framework that includes (i) downscaled climate forecasts, (ii) pavement performance predictions, and (iii) life cycle cost analysis. [Palin et al., \(2021\)](#) emphasize several major obstacles when it comes to assessing risks, including (i) managing uncertainties, understanding the relationships between weather impacts and railway infrastructure health conditions, (ii) evaluating the present and future costs of weather impacts, (iii) assessing the potential costs and benefits of adaptation. [Mitoulis et al., \(2023\)](#) proposed a framework for quantifying the trade-offs between sustainability and resilience for bridge assets and performed a comprehensive assessment of the performance and cost of transport infrastructure. They examined the impact of climate change on the sustainability and resilience indexes and showed how the optimum solutions are adversely affected by different climate projections.

The Cox proportional hazards model (PHM), [Cox, \(1972\)](#), is an appropriate approach that can be utilized to integrate the multiple climatic impacts (covariates) with RAMS (Reliability, Availability, Maintainability, and Safety) and LCC analyses to achieve more accurate LCC predictions. Several researchers used the PHM to develop reliability analysis by considering the effect of various covariates ([Bendell et al., \(1991\)](#); [Kumar et al., \(1992\)](#); [Kumar and Klefsjö, \(1994\)](#); [Barabadi et al., \(2014\)](#)). For instance, [Barabadi et al., \(2014\)](#) used the PHM to predict and optimize spare parts requirements. The study introduces a practical methodology that incorporates reliability models with covariates, illustrating its effectiveness in forecasting the demand for spare parts. [Mazidi et al., \(2017\)](#) proposed a hybrid approach based on Neural Network (NN) approaches and PHM where NN is utilized for real-time performance evaluation and PHM helps in real-time stress condition assessment. The hybrid model offers the possibility to evaluate wind turbine management policies and provides recommendations to improve maintenance strategies. Some of the latest research in this area is provided in [Table 1](#).

To the best of the authors' knowledge, utilizing PHM as a tool to integrate and assess the climatic impact on railway infrastructure assets has not been considered previously in the literature. The paper proposes an LCC methodology to evaluate the impact of climatic parameters, e.g., temperature, precipitation, wind speed, and relative humidity on LCC under various future climate scenarios, including Shared Socioeconomic Pathways (SPPs). The proposed model integrates weather covariates with operation and maintenance parameters (RAMS parameters) to predict climate change impacts on asset behavior and future demand.

The rest of the paper follows: [Section 2](#) explains the background and prerequisites. The impacts of climate change in the northern region of Sweden are discussed in [Section 3](#). The proposed methodology is presented in [Section 4](#). [Section 5](#) presents the results with a short discussion of the implications of the proposed methodology of the selected use case. The conclusion of this study is provided in

**Table 1**  
Some of the latest papers on the application of PHM in maintenance.

Reference	Short description
<a href="#">Thijssens and Verhagen, (2020)</a>	Evaluated the use of an extended Cox PHM in analyzing time-on-wing data of aircraft components, finding that it provides a more accurate prediction of time-to-failure than traditional survival analysis methods.
<a href="#">Liu, B. et al., (2020)</a>	Used PHM to develop a maintenance strategy considering system components' aging and cumulative damage.
<a href="#">Chen et al., (2020)</a>	Combined the Cox PHM with deep learning (DL) techniques to improve the accuracy of maintenance predictions.
<a href="#">Zheng, H. et al., (2021)</a>	Proposed a PHM involving degradation trends and environmental factors to predict product reliability.
<a href="#">Zheng, R. et al., (2023)</a>	Introduced a new hybrid model for repair and replacement, which integrates the PHM with a stochastically increasing Markovian covariate process.
<a href="#">Kasraei et al., (2024)</a>	Integrating the condition health of railway assets with meteorological data through PHM. Utilizing machine learning for clustering the railway network into four distinct areas.

## Section 6.

## 2. Background

This section briefly describes the three main aspects of the study: Switches and Crossings, LCC formulation, and Cox Proportional Hazard Model.

## 2.1. Switches and crossings (S&amp;C)

S&C is a critical asset in railway networks, which has a great impact on the railway network's capacity and availability. The S&C can be technically divided into three major panels: switch, closure, and crossing panels (see Fig. 1). The main components of S&C include switch rails, stock rails, crossings, wing rails, point machines, rail pads, sleepers, switch rollers, heating devices, and slide plates. In this paper, all these components have been categorized into four categories: Switch, Point Machine, Crossing, and Heating Device. As can be seen in Fig. 1, the switch blades, front joint, and other components in the switch panel, except the Switch drivers, are included in the Switch category. The category of point machines involves switch drivers in this panel. All Closure and Crossing panels components are in the Crossing category. The heating device includes heating elements on rail sides in S&C and other electrical assets.

## 2.2. LCC formulation

The LCC formula for an asset includes the costs associated with the design, production, installation, operation and maintenance (O&M), and disposal of the S&C asset over its expected lifespan. There are several formulas for calculating LCC, and we have followed the LCC formula given in (Nissen, (2009); Galar et al., (2017); Ebeling, (2019)) see Equation (1):

$$LCC = \text{Acquisition Costs} + \text{Operation and Support Costs} + \text{Phase-out Costs} \quad (1)$$

where

- **Acquisition Costs:** include the costs of design, fabrication, production, manufacture, installation, and other costs related to the development stage.
- **Operation and Support Costs:** include the cost of operations, maintenance (inspections, repairs, and replacements), support, and failure costs during the operational life of the asset.
- **Phase-out Costs:** net salvage value, which includes residual or salvage value, dismantling cost, and disposal cost.

Acquisition and phase-out costs are considered to be fixed within the context and scope of this study. Thus, this research focused on the operation and support costs of the LCC formula. Operation and support costs can include activities such as regular monitoring and inspections, cleaning, lubrication, repair, and other actions of the S&Cs. The frequency and intensity of maintenance activities can depend on several factors, including the design life of S&C, the layout of the track, the materials used, the environmental conditions, speed, and the traffic volume. This paper focuses on some corrective maintenance actions with high frequencies of intervention.

## 2.3. Cox Proportional Hazard Model

The Cox PHM is a statistical technique used to analyze the time-to-event data, where multiple factors influence the occurrence of an event. It assumes that the hazard rate, which represents the probability of experiencing the event at any given time, is a function of covariates or predictor variables. The model estimates the relative risk or hazard ratio associated with each predictor. This model was used to analyze the significant climate parameters influencing S&C performance. This model assumes that the hazard function can be separated into a baseline component and exponential functions associated with the explanatory variables, also called covariates

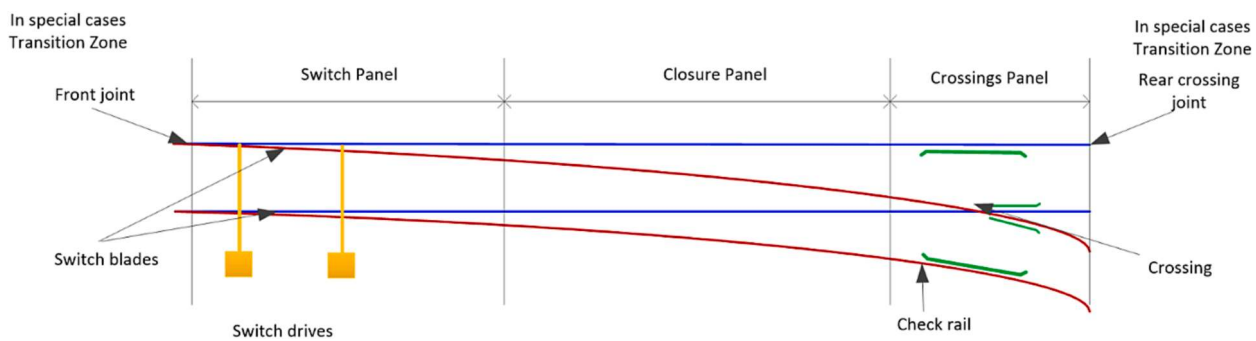


Fig. 1. Schematic presentation of S&C asset(Mishra et al., (2017)).

(Bendell et al., (1991)). Equation (2) illustrates the hazard model formula for the Cox PH model.

$$h(t, \mathbf{X}) = h_0(t) e^{\sum_{i=1}^p \beta_i X_i} \quad (2)$$

Where  $\mathbf{X}$  is the predictor vector variable. Hazard ratio (HR) represents the hazard for an asset divided by the hazard for another asset, where the assets being compared differ in their predictor values, denoted by  $X_1$  and  $X_2$  see Equation (3).

$$HR = \frac{h(t, \mathbf{X}_2)}{h(t, \mathbf{X}_1)} = \frac{h_0(t) e^{\sum_{i=1}^p \beta_i X_{2i}}}{h_0(t) e^{\sum_{i=1}^p \beta_i X_{1i}}} = e^{\sum_{i=1}^p \beta_i (X_{2i} - X_{1i})} \quad (3)$$

### 3. Climate change and its impact on the North region in Sweden

Swedish transport administration divided the whole railway network into five operations and maintenance areas, as given in Fig. 2. This section focuses on Luleå and Kiruna cities, which are both located in the North region.

#### 3.1. Analysis of weather parameters in some areas in the North region

The impact of climate change is already evident through various observable phenomena, such as an increase in extreme weather events like heat waves, floods, and storms. It is important to note that climate change affects different regions unequally. There are a lot of models and databases that investigate climate change's effects all over the world. In this study, we focus on the North region. We have illustrated the effects of climate change on the Luleå and Kiruna cities, as shown in Figs. 2, 3, and 4. The utilized data originated from ERA5, the fifth-generation European Centre for Medium-Range Weather Forecasts (ECMWF) atmospheric reanalysis of global climate patterns, covering the period from 1979 to 2021, with a spatial resolution of 30 km (Meteoblue, (2023)).

Fig. 3-a and Fig. 3-b show an approximation of the average annual temperature for Luleå and Kiruna, respectively. The dashed blue line represents the linear trend of climate change. The trend line slopes upwards from left to right, indicating a positive temperature trend, signifying that Luleå and Kiruna are experiencing warmer conditions due to climate change for a given period. In the lower section of the graph, you can see the representation of warming stripes. Each colored stripe corresponds to the average temperature for a particular year, with blue colors denoting years colder than the average of 1979–2021 and red representing warmer years.

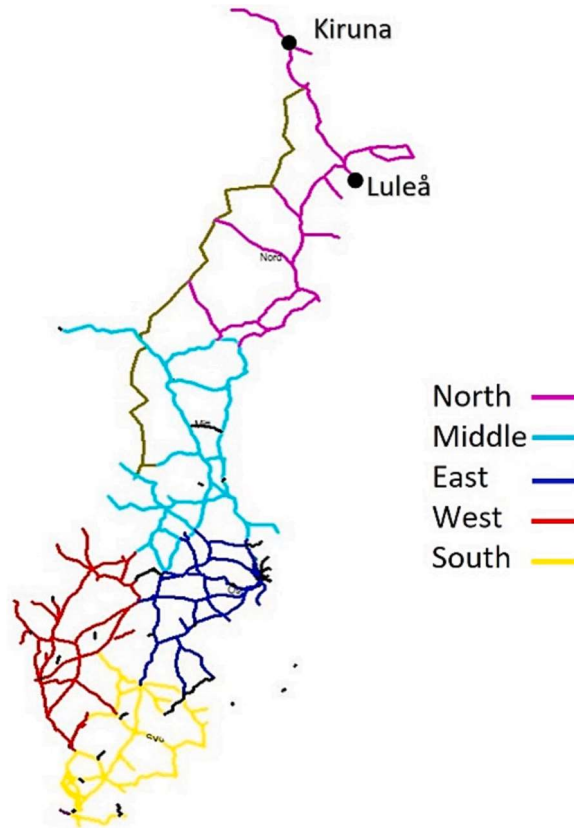
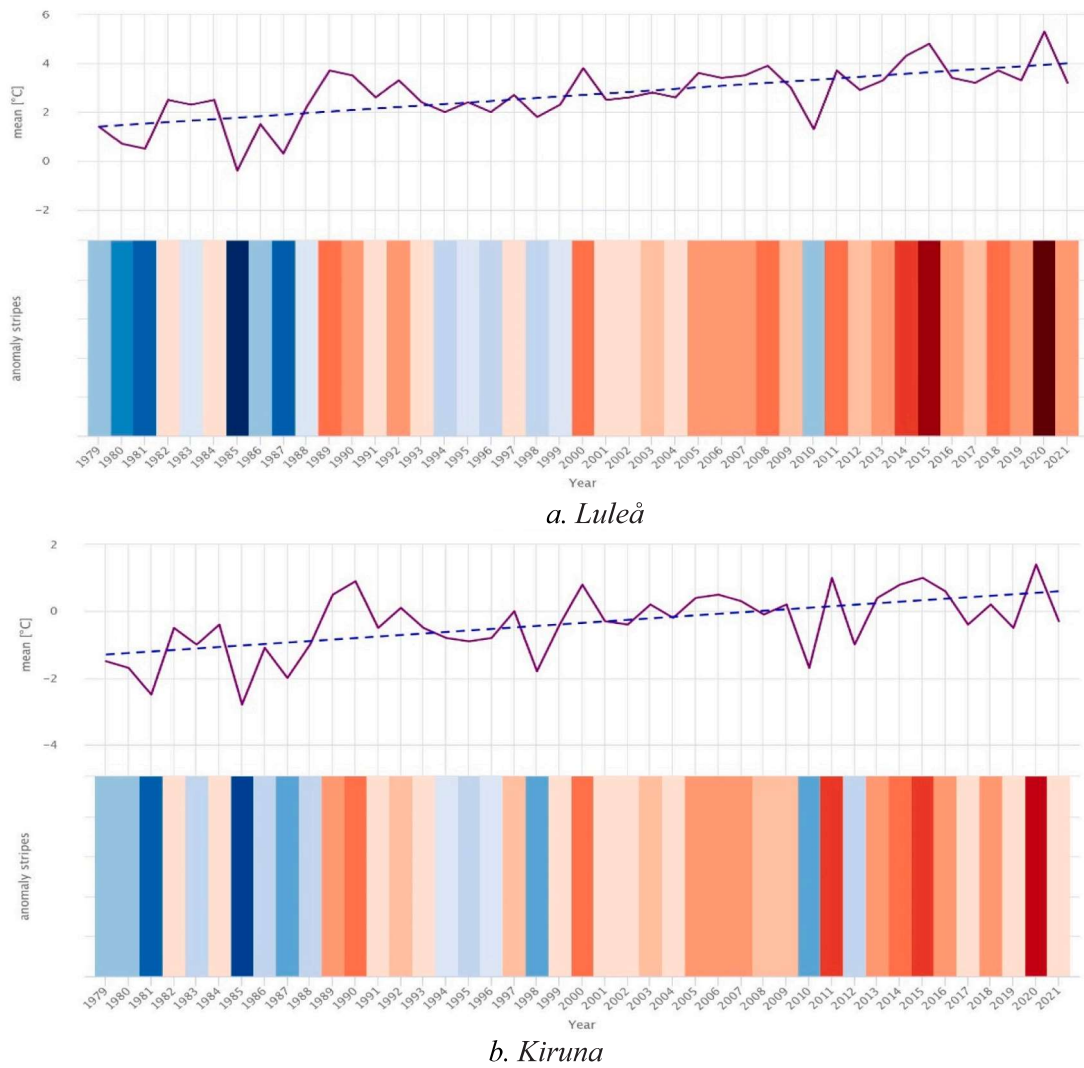


Fig. 2. Region's railways of Sweden.



**Fig. 3.** Yearly Temperature Change (Meteoblue, (2023)).

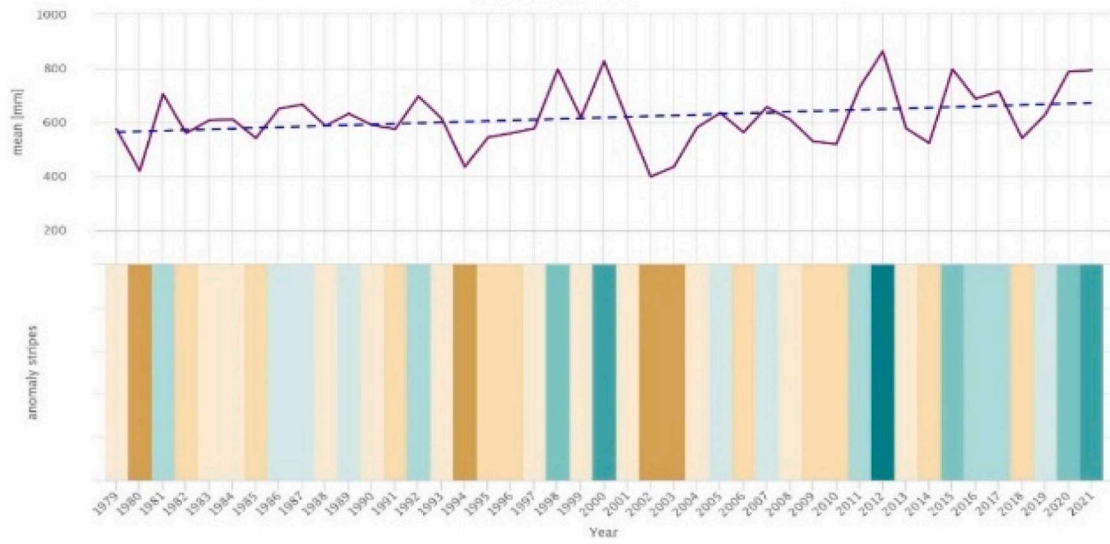
Fig. 4-a and Fig. 4-a present an estimation of the average total precipitation for Luleå and Kiruna cities. The dashed blue line represents the linear trend of climate change. The trend line slopes upwards from left to right, indicating a positive precipitation trend, suggesting that these cities experiencing increased rainfall over time due to climate change. In the lower section of the graph, you can observe the representation of precipitation stripes. Each colored stripe corresponds to the total precipitation of a particular year, with green denoting years wetter than the average of 1979–2021 and brown representing drier years.

Based on the above explanation, it can be observed that the temperature in this region shows an increasing trend over time, and there is also a rise in annual precipitation during the studied period. Understanding the current and future weather impacts can assist transport infrastructure managers in selecting the most effective strategy to mitigate the associated risks. For this purpose, RCP and SSPs climate change scenarios have been developed. These scenarios are explained in Section 3.2. It is important to note that climate change scenarios are not intended to predict the future but to provide projections of potential outcomes or pathways to achieve specific goals.

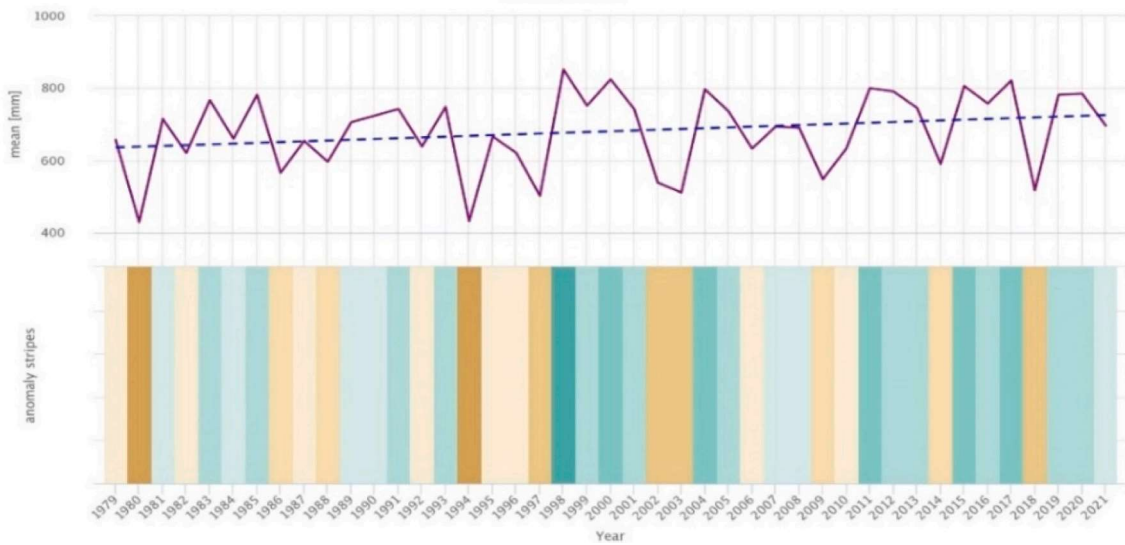
### 3.2. Climate change projection scenarios for North region

There are two kinds of climate change projection scenarios: Representative Concentration Pathways (RCPs) and Shared Socio-economic Pathways (SPPs). In these scenarios, the focus is primarily on long-term trends in global climate and greenhouse gas emissions. However, the effects of climate change can be seen in changes to local weather patterns and extreme weather events, such as heatwaves, droughts, floods, and storms.

RCPs proposed by UN Climate Panel IPCC5 knowledge can be used to project future climate changes. Four RCP scenarios, RCP2.6,



a. Luleå



b. Kiruna

Fig. 4. Yearly Precipitation Change (Meteoblue, (2023)).

RCP4.5, RCP6, and RCP8.5, have been considered, which differ in their assumptions about future climate scenarios. Furthermore, SSP scenarios describe different socioeconomic developments, considering the influence of climate change scenarios (O'Neill et al., (2014)). The five SSP scenarios are defined as SSP1 (Sustainability), SSP2 (Middle of the Road), SSP3 (Regional Rivalry), SSP4 (Inequality), and SSP5 (Fossil-Fueled Development). Fig. 5 illustrates the precipitation projection of these scenarios for North in Sweden based on a multi-model ensemble. The precipitation trend in both RCP and SSP scenarios shows an increasing amount of precipitation in a long-term period.

Based on findings from prior research (Garmabaki and Kumar, 2019), Fig. 6 illustrates the anticipated winter temperature projections for Luleå and Kiruna across various RCP scenarios. The results demonstrate a consistent rise in temperature in all scenarios. For instance, in the Luleå area, comparing the period 2011–2040 to 1971–2000, there is an increase of almost 4 degrees Celsius under the RCP8.5 scenario. Furthermore, the temperature increment for the period 2071–2100 compared to 2011–2030 is particularly noteworthy, with a peak approaching 5 degrees Celsius under the RCP8.5 scenario. This upward trend is concerning, as it has the potential to impact critical factors such as zero crossing and an elevated likelihood of climatic failures. Meanwhile, Fig. 7 depicts the projected increase in summer temperatures for Luleå city during the 2071–2100 period compared to 2011–2030, indicating a rise of approximately 4 degrees Celsius.

Fig. 8 illustrates the projected winter precipitation for Luleå and Kiruna based on various RCP scenarios. Our results indicate a rise

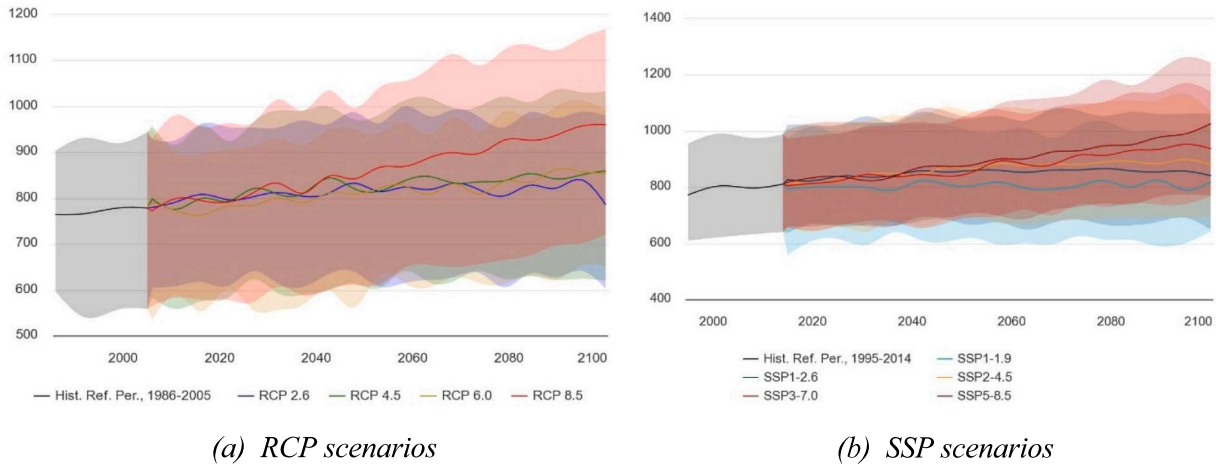


Fig. 5. Projected precipitation for North in Sweden (World Bank Group, (2021)).

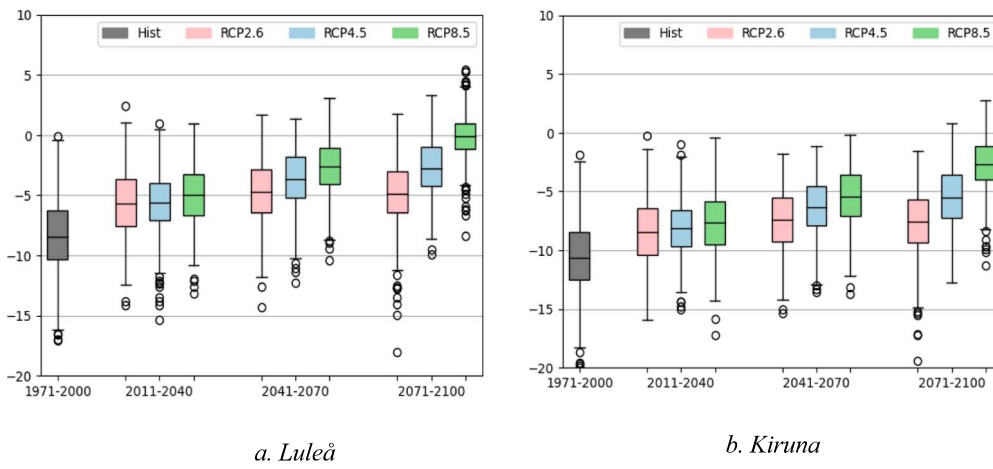


Fig. 6. Projected winter temperature ( $^{\circ}\text{C}$ ) in two Swedish cities in the historical period 1971–2000 grey boxes, and the periods 2011–2040, 2041–2070, and 2071–2100 according to RCPs. The boxes represent the interquartile range (IQR) of the data, the line within represents the median, and the whiskers extend from the box by  $1.5 \times \text{IQR}$ . Data points outside the whiskers are marked by circles.

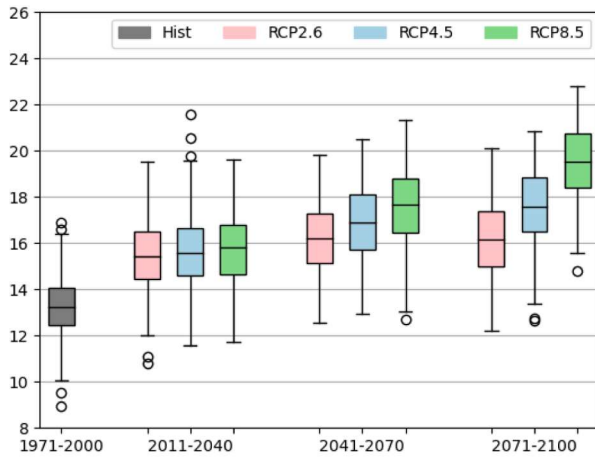
in precipitation across all scenarios. Also, the summer precipitation is projected to increase and is a relatively small change compared to winter precipitation (see Fig. 9). Furthermore, there is a negligible change in summer precipitation over RCP2.6 scenario.

#### 4. Methodology

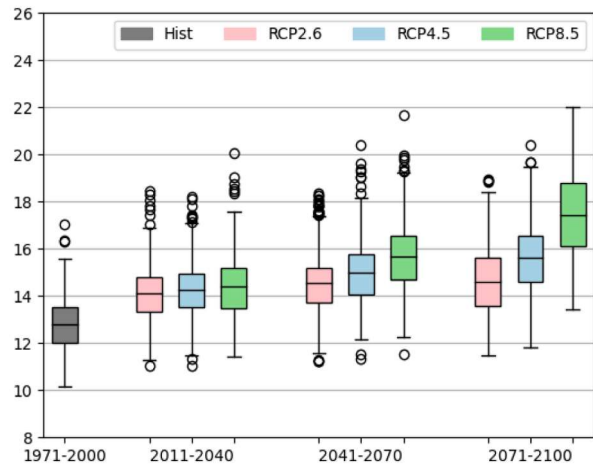
The paper proposes a methodology to assess the impact of climatic parameters, e.g., temperature, precipitation, and relative humidity, on LCC of railway infrastructure assets under various future climate scenarios, including SSP1-SSP5. The proposed model integrates weather covariates with operation and maintenance parameters (RAMS parameters) to predict the impact of climate change on asset behavior and LCC. Our research focus is limited to considering the above-mentioned climatic impacts on the number of S&Cs located in the North region of Sweden. To perform this task, the proposed methodology utilizes Cox PHM to integrate weather covariates with operation and maintenance parameters (RAMS parameters) to predict the impact of climate change on the LCC of the assets.

Fig. 10 depicts the proposed framework, including the following five steps:

- Data collection,
- Data preprocessing and filtering,
- Development of LCC model with RAMS parameters,
- Impact modeling of climate change on LCC,
- LCC analysis based on different SSP scenarios.

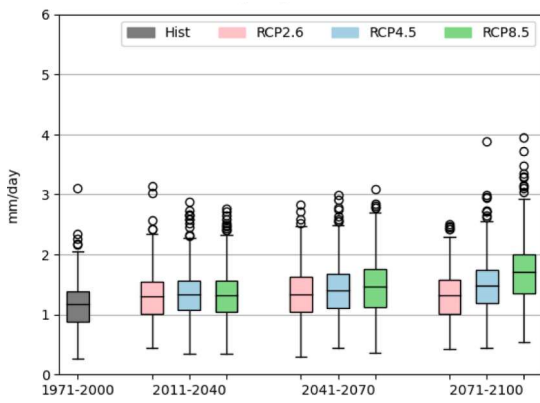


a. Luleå

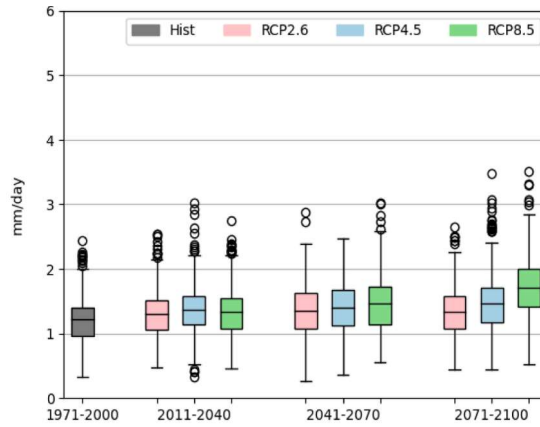


b. Kiruna

Fig. 7. Projected summer temperature (°C) in two Swedish cities.



a. Luleå



b. Kiruna

Fig. 8. Projected winter precipitation (mm/day) in two Swedish cities in the historical period 1971–2000 grey boxes, and the periods 2011–2040, 2041–2070, and 2071–2100 according to RCPs.

Due to the stochastic nature of the failure events, the proposed methodology focuses on corrective maintenance actions; therefore, acquisition costs, preventive actions, and phase-out costs were not considered in the LCC analyses.

#### 4.1. Step1: Data collection and Data analysis

The data for this study was gathered from multiple data sources, including the Ofelia database (failure reporting system), which records all infrastructure failures, and the BIS database (asset registry), which provides information on failed assets for 18 years 2001–2018. VViS (The Swedish Transport Administration's weather information database) and SMHI databases (SMHI, (2023)) have been used to collect weather parameters and associated climate measures. There is a need to combine the various railway databases, including Ofelia, BIS, and SMHI databases, to extract climate features, namely Climate\_id. This indicator identifies the causal relationship between S&C failures and climate parameters at the time prior to failure (Garmabaki and Kumar, (2019)). All the climate-based and non-climatic failures have been extracted by text mining technique, failure causes code, experts' opinions, etc.

For the study, the variations in temperature, precipitation, and humidity for the Norrbotten region associated with various SSP scenarios have been collected from the World Bank webpage (World Bank Group, (2021)).

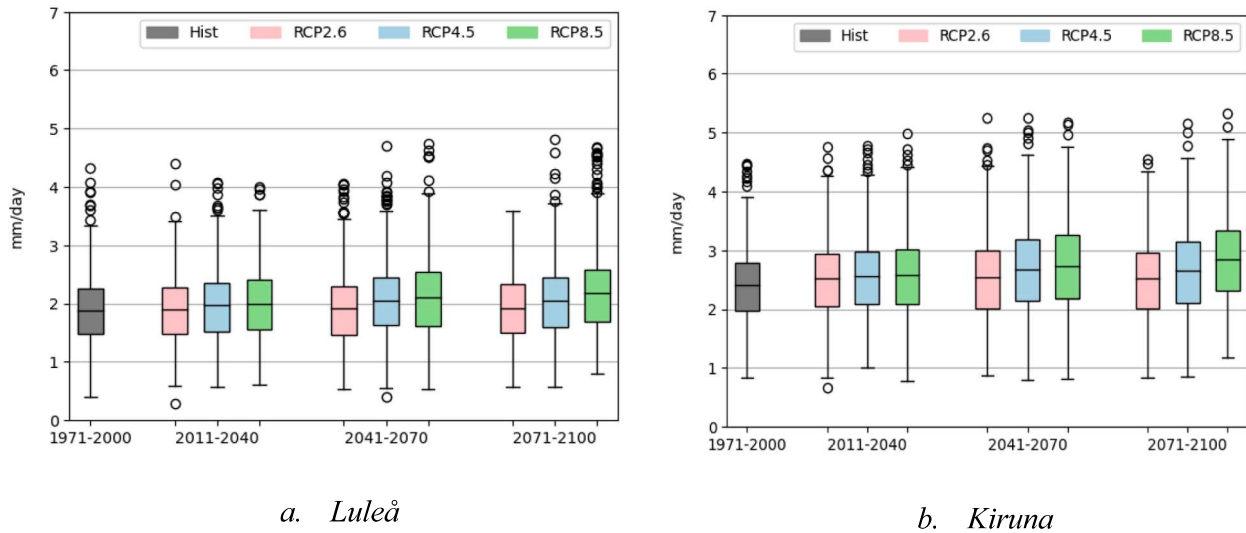


Fig. 9. Projected summer precipitation (mm/day) in two Swedish cities.

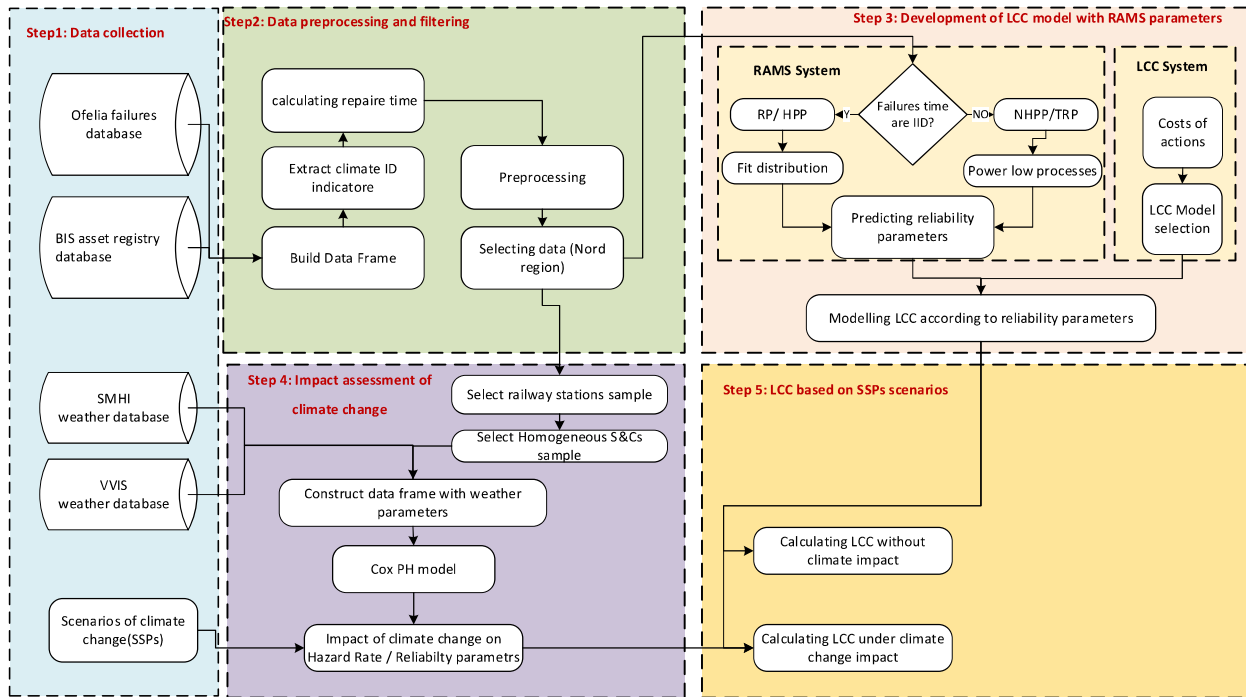
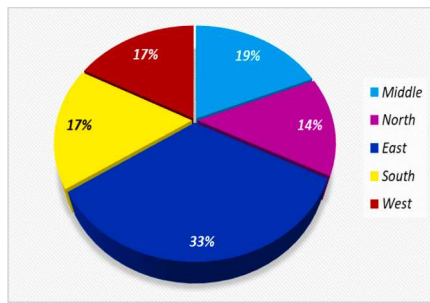


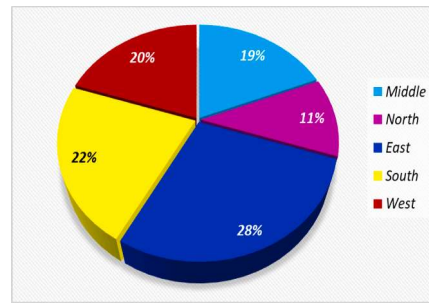
Fig. 10. Framework of workflow.

#### 4.2. Step 2: Data preprocessing and filtering

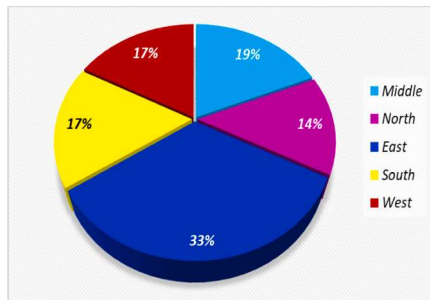
The preprocessing task was conducted to improve the dataset's quality by removing anomalies and cross-validation of failure with weather incidences. This phase includes data cleaning (such as handling missing data and outliers), data integration to unify the data that comes from multiple sources, and visualizing data to gain insights and identify patterns and relationships in data. The distribution of all the failures across different regions in Sweden is illustrated in Fig. 11-a, and the number of S&C assets in each district is displayed in Fig. 11-b. The proportion of non-climate and climate-related failures in various regions of Sweden was depicted in Fig. 11-c and Fig. 11-d, respectively. For this research, the North area of Sweden was selected as a use case. The assets in the North region account for 11 percent of the total assets and contribute to 25 percent of climatic failures; therefore, the North region is selected for the use-case. To improve accuracy, only failures with a repair time of less than 480 min were included in the analysis, as recommended by experts. This



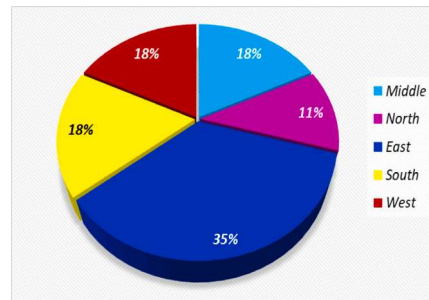
a. Distribution of failures in different regions



b. Distribution of S&amp;C assets in different regions



c. Distribution of climatic failures in different regions



d. Distribution of Non-climatic failures in different regions

**Fig. 11.** Distribution of Regions.

decision was made based on two reasons, including (i) Due to redundancy S&Cs in the railway yard, the failed asset may not receive immediate prioritization, and (ii) Climate-related failures typically require short repair and maintenance times (less than 480 min), only common and not extreme incidences are considered here.

This study focuses on operational costs associated with repair and maintenance actions of 1258 S&C. Thus, some maintenance actions are considered, including Snow cleaning, Cleaning, Repair, Washing, Lubrication, Control, Adjustment, and Recovery. The percentage of these actions can be seen in Table 2. By analyzing this data, we can better understand the specific actions that are most frequently performed and identify potential areas for potential improvement in terms of reducing operational costs and improving dependability and comfort performance. According to available data, Snow cleaning (as an action with the highest frequency) has the highest cost, about 35 %.

Fig. 12 illustrates the percentage of each action cost according to climatic or non-climatic mode. Snow cleaning, Cleaning, Washing, and Adjustment actions have higher costs in climatic mode, whereas Repair, Adjustment, Control, and Lubrication have higher costs in non-climatic mode.

The existing database has six essential categories of extreme weather conditions, including Abnormal temperature, Flood, Fire,

**Table 2**

Maintenance actions for climatic failure in Sweden.

Actions	Frequency Percentage	Action Description
Snow cleaning	41.88 %	Removal of snow and ice during the winter season
Cleaning	26.20 %	Remove debris, sand, stones, and other foreign objects in the S&C.
Adjustment	9.60 %	Correction of the geometric features or positional misalignment of S&C after standard measurement
Washing	9.47 %	Cleaning of turnout components using a fluid or other relevant medium.
Lubrication	4.12 %	Applying a substance such as oil or grease to S&C components to minimize friction and allow smooth movement.
Control	1.84 %	Gauging and functional check of the state of the system.
Repair	1.33 %	Maintenance actions are carried out to return S&C to a state where it can perform the desired function by replacing components, welding, and grinding.
Recovery (Restoration)	1.05 %	Resetting and returning the S&C component to initial or calibrated status after failure; performing regular standard operational procedures.
Other	4.06 %	All other actions, e.g., grinding, tamping, tightening, and etc.

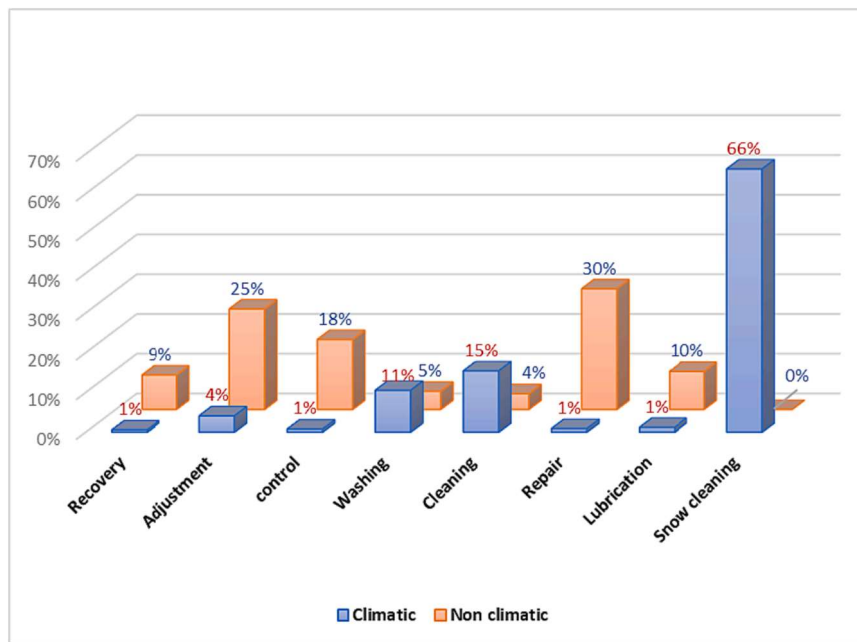


Fig. 12. Distribution of cost of actions in North zone.

Snow and Ice, Storm/snowstorm, and Thunderstorm. The major climatic factors contributing to failures in the North region are Snow and Ice, Abnormal temperature, and Storm/Snowstorms, whereas Fire, Flood, and Thunderstorms occur relatively less. Primary failure analysis in cross-validation with weather databases reveals that climatic failures constitute 53 % of all failures, while unknown and non-climatic failures account for the remaining 47 % of the North region. Fig. 13 presents the details of cost according to climatic and non-climatic failures. Notably, Snow and Ice contribute to 83.3 % of the total cost of climatic failures, emphasizing the significance of implementing measures to mitigate the impact of this failure cause in the region.

Fig. 14 illustrates the cost distribution associated with each maintenance activity across all defined components of the S&C system. This figure will help better understand the critical S&C components and provide insight for infrastructure managers regarding resource

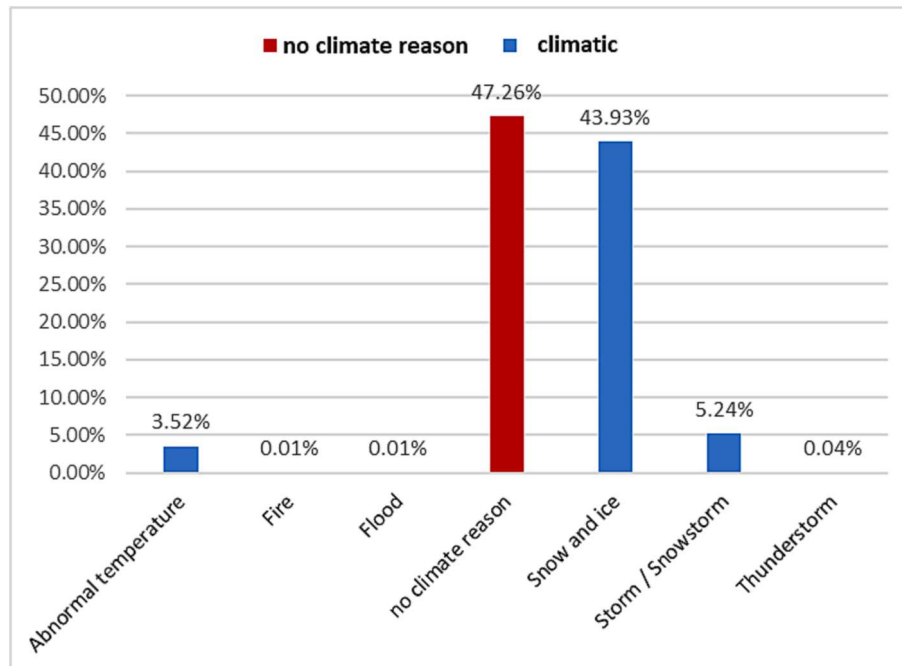


Fig. 13. Cost according to Climate ID indicator.

allocation and maintenance planning, leading to improved dependability performance.

#### 4.3. Step3: Identification model for LCC with RAMS parameters

The maintenance and repair costs play the main role in LCC analysis. The present value of all costs throughout the expected lifespan of the S&C system is calculated by applying an appropriate discount rate, which accounts for the time value of money. The various actions taken to treat the fail component should be reflected in the LCC model. Due to their criticality and failure rate, we are just focusing on the switch, point machine, crossing, and heating system. The cost per action is one of the most challenging pieces of information to obtain when developing the LCC model. In this study, the cost is modeled using Equation (4):

$$LCC = \sum_k \sum_i \sum_j \frac{1}{(1+r)^k} \frac{1}{MTBF_{ij}(k)} \{C_{P_{ij}} + MTTR_{ij}(n_{L_{ij}}C_L + C_{E_{ij}})\} \quad (4)$$

Where  $i$  is the action type,  $k$  is the year's duration, and  $j$  is the component type.  $MTBF_{ij}(k)$  is the Mean-Time-Between-Failure of component  $j$  and a failure mode associated with action  $i$  for year  $k$ th;  $MTTR_{ij}$  is the Mean-Time-To-Repair of component  $j$  (in minute units) and a failure mode associated with action  $i$ ;  $n_{L_{ij}}$  is the number of workers needed for a given action;  $C_P$  is the cost of the spare part (in monetary units);  $C_L$  is labor cost (in monetary units/hour); and  $C_E$  is the equipment cost needed to carry out the intervention.

MTBF and MTTR are two important key performance indicators that need to be estimated for action  $i^{th}$  and component  $j^{th}$ . MTTRs are estimated, and results are shown in Table 3 for the given period. To estimate MTBF, the trend test is utilized at the first step for determining underlying processes e.g., HPP, RP, and NHPP. Trend-free behavior should be modeled by HPP or RP, while data with trend should be modeled with a nonhomogeneous Poisson process such as the power-law process. In other words, a trend test is carried out to see if the cumulative failure time significantly increases or decreases over calendar time.

Fig. 15 represents Mean Cumulative Function (MCF) over cumulative failure time of the Snow cleaning action (action  $i$ th) and Switch component (component  $j$ th). Use this plot to determine whether your system is improving, deteriorating, or remaining constant. It is evident in Fig. 15 that there is a gradually increasing trend in the curve over time. This increase indicates that the system is becoming less reliable or efficient over time.

The trend test analysis given in Table 4 confirms the interpretation of the above curve, and the P-value indicates that the null hypothesis of all trend tests is rejected. This means NHPP should be followed to estimate MTBF.

It may be noted that, in MIL-Hdbk-189 and Laplace trend tests, the null hypothesis is “No trend” ( $H_0$ ) versus the alternative hypothesis of “Monotonic trend”. The Anderson–Darling test (AD) rejects the null hypothesis ( $H_0$  is “No trend”) in the presence of both monotonic and non-monotonic trends when the value of AD is large (Garmabaki et al., (2016)).

Fig. 16 shows the graphical behavior of the cumulative failure time of the Control action for the switch component. The trend test analysis confirms that cumulative failure time is trend-free, as given in Table 5 (the P-value is greater than 0,05). Thus HPP/RP are suitable modeling approaches for this action. Furthermore, Fig. 17 shows the graphical goodness-of-fit-test of selected distributions. For all the actions performed on the prespecified four components, the estimated parameters, along with the appropriate process, have been listed in Table 6.

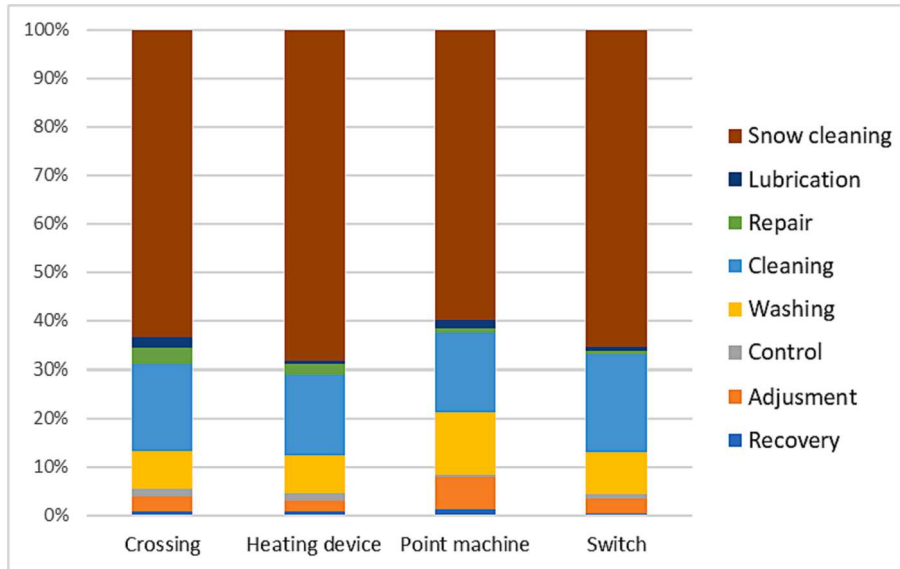
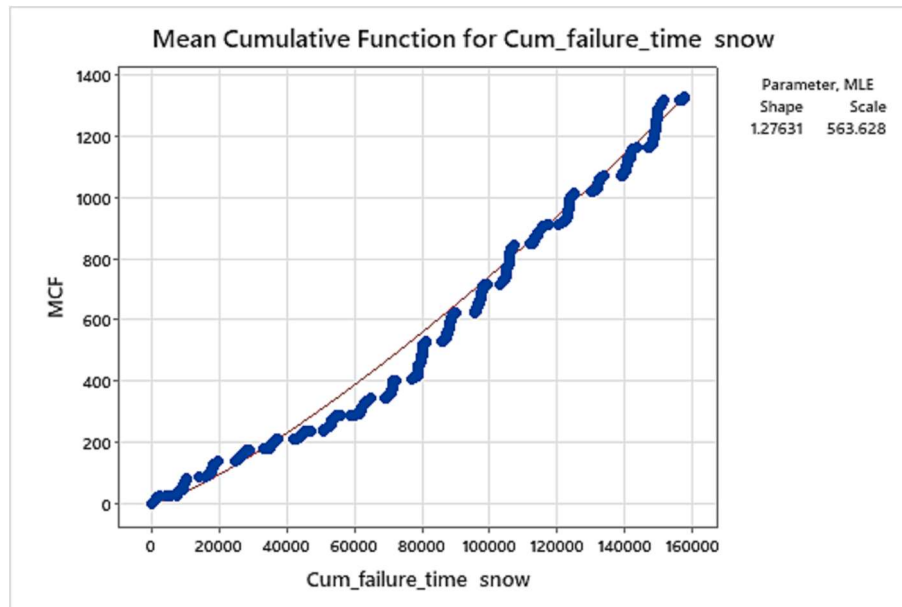


Fig. 14. The cost of actions for each part of S&C related to climatic failures.

**Table 3**  
Mean Time To Repair.

Actions	Switch	Crossing	Point Machin	Heating Device
Snow cleaning	71.108	87.305	66.05	71.262
Adjustment	65.828	126.72	68.783	76.645
Control	52.483	48.729	50.397	57.859
Repair	110.821	184.306	115.629	102.375
Recovery	65.348	121.758	84.623	65.471
Cleaning	56.633	57.945	56.823	57.121
Washing	64.331	57.624	63.877	66.707
Lubrication	52.341	42.06	55.261	48.225



**Fig. 15.** Graphical demonstration of MCF versus cumulative failure time of snow cleaning for Switch component.

**Table 4**  
Trend test result for snow cleaning of switch.

	MIL-Hdbk-189	Laplace	Anderson-Darling
Test Statistic	2079.44	10.21	59.48
P-Value	0.000	0.000	0.000
Result	Rejected	Rejected	Rejected

#### 4.4. Step 4: Impact of Climate Change on Failure Hazard Rate by Cox-PHM

For Cox PH analysis, various covariates, including Temperature (T), Humidity (H), Precipitation (P), and failure time, have been selected. It is important to note that the effects of the selected weather covariates are not immediate but gradual. Therefore, the average hourly value of covariates during the 24 h preceding the failure event is calculated and used as input in the Cox PHM to reflect the meteorological effects. In the initial step, three stations from different geographical locations in the North region, which included 32 S&Cs, were selected. Bartlett's test is utilized for heterogeneity tests to identify homogenous S&C groups. The analyses presented in this paper are related to a selected homogenous group consisting of 9 S&Cs. For the details, see [Garmabaki et al., \(2016\)](#).

##### 4.4.1. Calculating baseline hazard function

At this stage, the baseline hazard function of the selected 9 S&C assets is determined for the Cox-PH model. The graphical and statistical trend tests are employed to assess the validity of the independent and identically distributed (IID) nature of TBFs of combined S&Cs. [Fig. 18](#) shows that the selected assets exhibit an obvious trend. Furthermore, statistical tests such as the Military Handbook, Laplace, and Anderson-Darling have also confirmed the findings of the graphical tests. Consequently, the Power Law model, which is a specific form of the NHPP, is utilized to construct the baseline. The parameters of the power law process, including

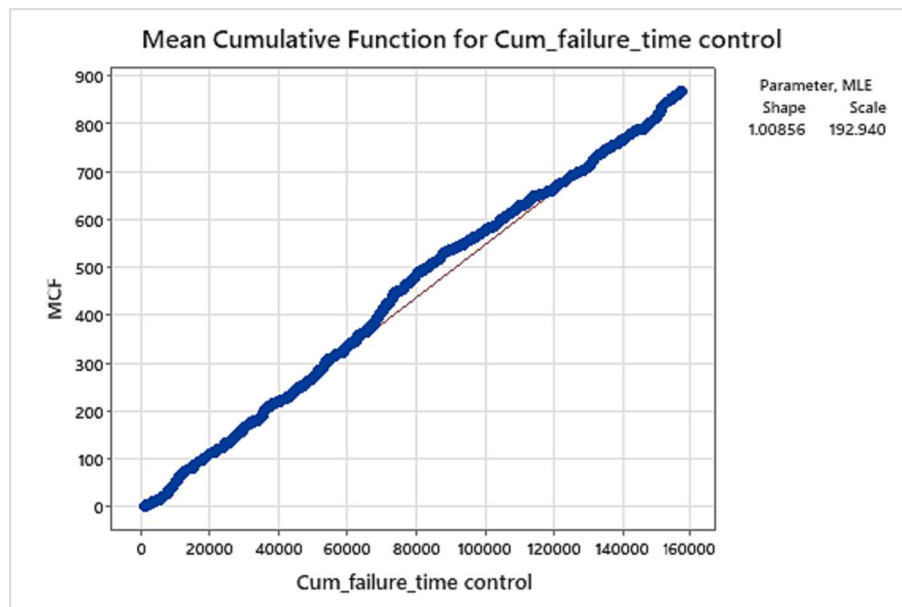


Fig. 16. Trend test for Control action for Switch part.

Table 5

Trend test result for Control Action for Switch.

	MIL-Hdbk-189	Laplace's	Anderson-Darling
Test Statistic	1717.30	-1.11	2.05
P-Value	0.838	0.268	0.086
Result	Not reject	Not reject	Not reject

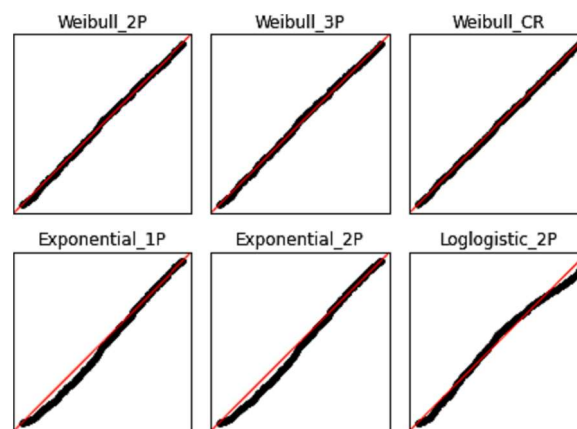


Fig. 17. Fitting distribution of Control Action.

shape ( $\beta$ ) and scale ( $\theta$ ), are estimated using Minitab software. The estimated shape and scale parameters for the selected homogenous group are 1.557 and 11423.1, respectively. Therefore, the baseline hazard rate function is as follows:

$$h_0(t) = \frac{1.557}{11423.1} \left( \frac{t}{11423.1} \right)^{0.557} \quad (5)$$

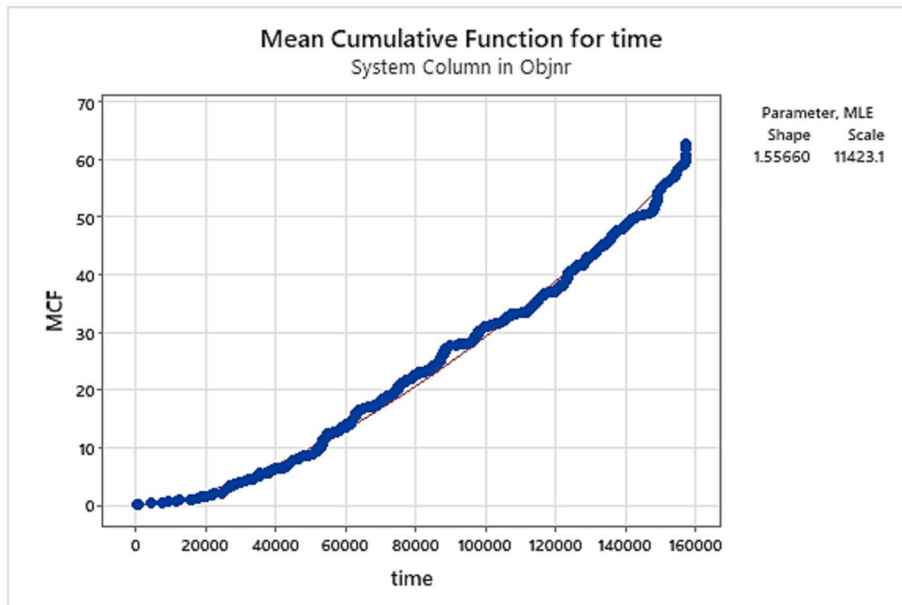
#### 4.4.2. Calculating the coefficients of covariates

The Andersen-Gill (AG) model has been used to assess the impacts of covariates on hazard rate. Table 7 displays the coefficients of the covariates and their corresponding hazard ratios (HR). The P-values in Table 8 indicate that the null hypothesis is rejected on a

**Table 6**

Trend test for all actions.

	Actions	Shape( $\beta$ )	Scale( $\theta$ )	t0	Distribution
Switch	Snow cleaning	1.276	563.628	0.516	NHPP
	Adjustment	0.758	18.73		NHPP
	Control	0.842	167.66		Weibull_2P
	Repair	0.883	238.315		Weibull_3P
	Recovery	1.441	3935.77	0.016	NHPP
	Cleaning	1.8	3384.41		NHPP
	Washing	0.559	166.472		Weibull_3P
	Lubrication	0.689	222.198		Weibull_3P
Crossing	Snow cleaning	1.226	3158.75	40.633	NHPP
	Adjustment	1.612	13195.2		NHPP
	Control	0.905	1400.9		Weibull_2P
	Repair	1.189	1466.03		NHPP
	Recovery	0.681	4378.99	0.583	Weibull_3P
	Cleaning	1.547	6298.56		NHPP
	Washing	0.698	1315.88		Weibull_2P
	Lubrication	0.637	1818.64		Weibull_3P
Point Machine	Snow cleaning	1.318	706.067	0.016	NHPP
	Adjustment	0.859	35.486		NHPP
	Control	0.805	168.911		Weibull_3P
	Repair	0.926	281.635		Weibull_2P
	Recovery	1.464	3920.16		NHPP
	Cleaning	1.69	2914.89		NHPP
	Washing	1.088	341.401		NHPP
	Lubrication	1.332	1386.38		NHPP
Heating Device	Snow cleaning	1.6031	4408.31		NHPP
	Adjustment	0.662	578.322		Weibull_2P
	Control	1.174	1202.24		NHPP
	Repair	0.668	413.109		Weibull_2P
	Recovery	1.409	2701.32		NHPP
	Cleaning	1.842	8349.72		NHPP
	Washing	1.5	7883.94		NHPP
	Lubrication	1.641	12646.9		NHPP

**Fig. 18.** Failure behaviour of the assets.

significant level of 10 % for all the covariates, implying that covariates significantly impact the hazard ratio.

Hence, according to Cox PHM and Equation (2), the hazard rate equation is presented in Equation (6):

$$h(t, \mathbf{X}) = h_0(t)e^{(-0.0212T - 0.0212H + 1.902P)} \quad (6)$$

**Table 7**  
Results of Cox PH model.

Covariate	Coef./ $\beta_i$	HR	P-value*
Temperature (T)	-0.0212	0.979	0.069
Precipitation (P)	1.902	6.699	0.046
Humidity (H)	-0.0212	0.979	0.002

\* The null hypothesis is “no significant effect on the hazard rate”.

**Table 8**  
The combined impact of precipitation, humidity, and temperature on hazard rate.

Year	SSP1-1.9	SSP1-2.6	SSP2-4.5	SSP3-7	SSP4-8.5
19	0.102723	0.110398	0.126578	0.12081	0.123696
20	0.102972	0.109895	0.125938	0.120453	0.124351
21	0.104766	0.110891	0.125456	0.119569	0.124691
22	0.107183	0.113321	0.124652	0.11868	0.124914
23	0.110498	0.115876	0.123747	0.117609	0.12403
24	0.113806	0.118411	0.122721	0.116896	0.123179
25	0.116665	0.119603	0.121792	0.11613	0.12161
26	0.118159	0.119304	0.120461	0.115612	0.11904
27	0.118506	0.117004	0.119418	0.115785	0.115981
28	0.117393	0.113987	0.118153	0.116031	0.112799
29	0.115222	0.1106	0.116867	0.115948	0.109863
30	0.112154	0.108127	0.115998	0.116086	0.107069

where  $h_0(t)$  is according to Equation (5).

Based on collected 18-year meteorological data, weather baselines are calculated based on the average values of temperature  $T_{av} = -1.54$  °C, humidity  $H_{av} = 81.57$  %, and precipitation  $P_{av} = 0.057$  mm. Fig. 19 represents the weather baseline (blue curve) and the hazard rate affected by selected weather parameters (red curve) in accordance with the values  $T = -1$ ,  $H = 78$ , and  $p = 0.096$ . The difference between these two curves signifies the impact of the weather parameters on the hazard rate function.

Through this method, we're able to assess and represent the influence of SSP scenarios on the hazard rate, which is further implemented for the estimation of LCC.

The projected values for temperature, precipitation, and humidity for the North region under various SSPs scenarios have been derived from the World Bank webpage (World Bank Group (2021)).

Fig. 20 reveals the increasing temperature and precipitation trends under SSPs scenarios, whereas the humidity trend is decreasing. To assess the yearly impact of these parameters on the hazard rate, Equation (2) has used the annual variations. Additionally, we compared these values with the weather baseline (blue curve in Fig. 19) to calculate the percentage of variation of the hazard rate for each SSPs, annually. To calculate new hazard rate capturing SSPs feature, there is a need to extract the projected value for the associated SSP. For instance, in Scenario SSP1-2.6, for the year 26th, the projected values for temperature, precipitation, and humidity are 0.45, 0.0959, and 77.75 %, respectively. By substituting these parameters into Equation (7), we estimated the new hazard rate, and then by comparing it with the baseline, we can estimate the variation of the hazard rate, which is 11.9 %. In other words, the impact of exogenous factors on LCC, which in our context is climate change impacts, is calculated from PHM and shown in Table 8 for each

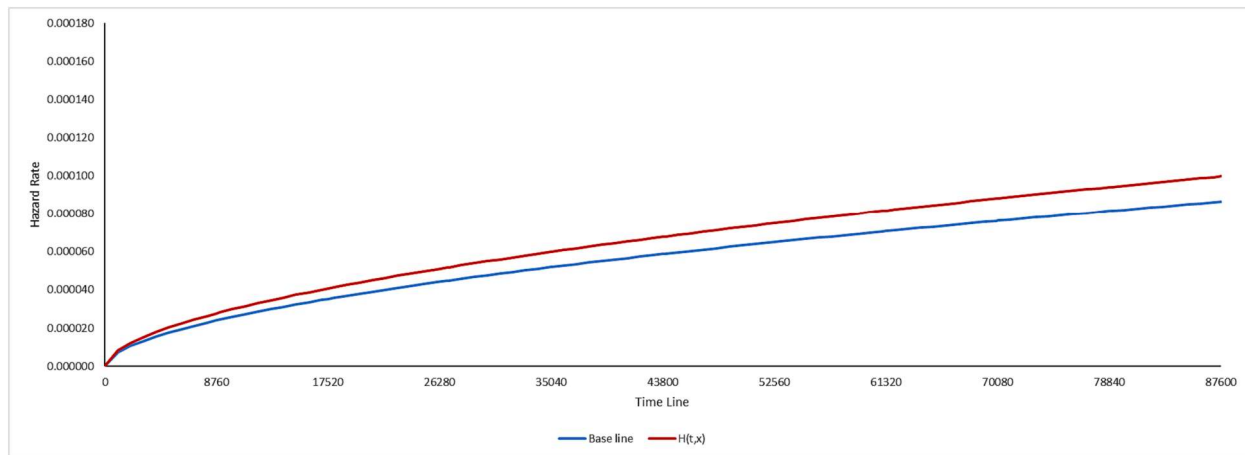


**Fig. 19.** Impact of covariates on Hazard function.

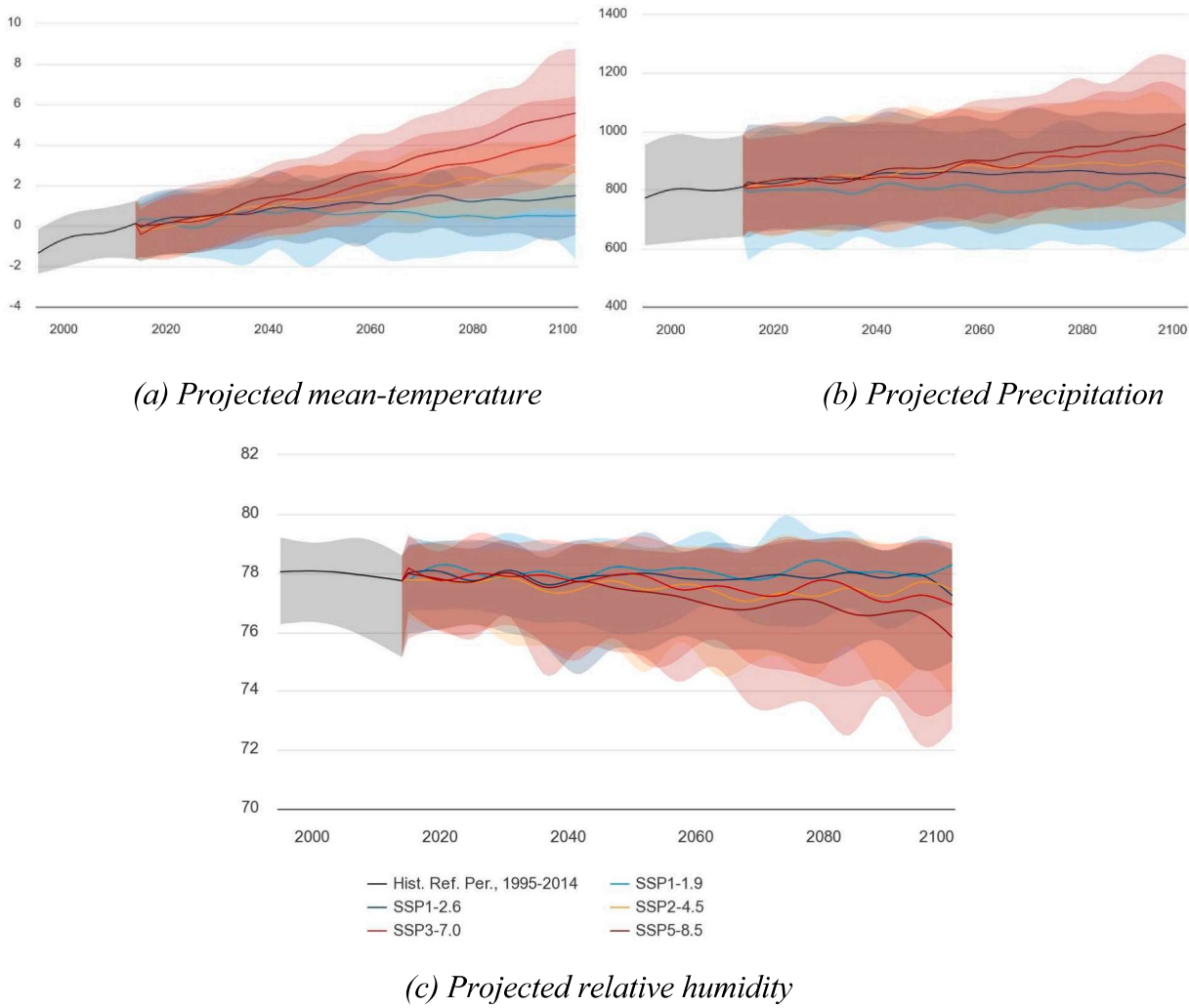


Fig. 20. Projected some parameters in North of Sweden (World Bank Group (2021)).

scenario.

#### 4.5. Step 5: LCC based on SSP scenarios

In this paper, we applied two approaches to evaluate LCC, including (i) LCC without climate change impacts and (ii) LCC under climate change impacts. Utilizing these distinguished approaches enables us to compare the impact of SSP scenarios on LCC.

In the first approach, LCC is calculated using Equation (4) in 30 years. Historical data for the duration of 18 years beginning from 2001 have been used for the LCC-RAMS model to estimate LCC for the next 12 years.

In Equation (4),  $C_L = 850$  SEK per hour,  $n_L = 2$  labor,  $C_E = 4,000$  SEK per hour for snow-cleaning action, and  $C_F = 1000$  SEK per hour for other actions. In this study, we suppose  $C_p = 0$  due to the low frequency of spare parts in climatic failures. Fig. 21 shows the evolution of the cost of maintenance in this period. As can be seen, *Snow Cleaning* shows the highest portion of the total cost over the mentioned period, and 'Cleaning' has the next rank because these actions have a high frequency among climatic failures.

In the second approach, the impact of hazard rate variations can be calculated through the amount of climatic impact (negative or positive impact/value in  $\gamma$ ) on the MTBF of selected assets per action evaluated from PHM. Negative impact can be interpreted as reduced climatic failure, while positive impact intensifies the failure occurrence. We have considered the additive mathematical form, as given in Equation (7), to assess the impact of SSP scenarios and estimate the LCC.

$$LCC_{SSP} = \sum_k \sum_i \sum_j \frac{1}{(1+r)^k} \left[ \frac{1}{MTBF_{ij}(k)} + \gamma_k \times \frac{1}{MTBF_{ij}(k)} \right] \left\{ C_{p_{ij}} + MTTR_{ij} (n_L C_L + C_{E_{ij}}) \right\} \quad (7)$$

where  $\gamma_k$  is positive/negative increment/decrement of selected impact for given SSP scenarios; see Table 8.

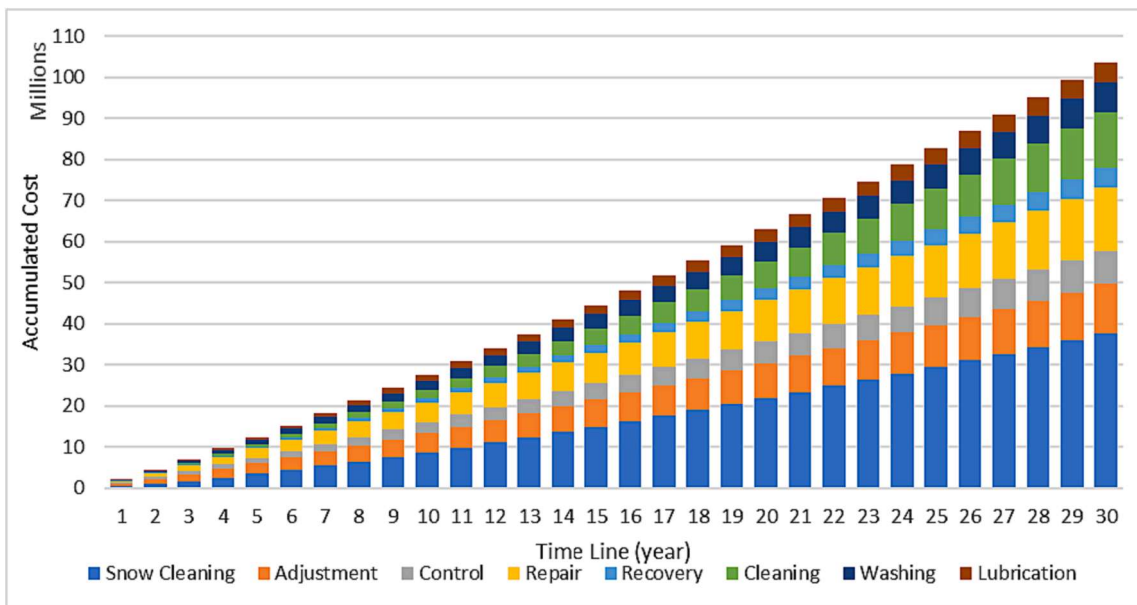


Fig. 21. Maintenance costs (LCC) in 30 years.

For instance, in Fig. 22, the LCC variation for 30 years is depicted under the SSP1-1.9 scenario. The blue bar represents the LCC without considering the impact of climate change parameters, while the orange bar represents the LCC when the impact of climate change parameters is considered (orange bar as approach 2) compared with LCC without considering climate impacts (blue bar as approach 1).

To have clear understanding of climate on maintenance actions, there is a need to categorize the LCC per maintenance actions defined in section 4.2 for different scenarios. Fig. 23 presents the cost of the different actions for the SSP1-1.9 scenario. Our analyses show that snow cleaning costs include 34 to 37 percent of the total cost over 30 years, and repair action costs vary between 14 and 16 percent.

In Fig. 24, the LCC under SSP 2-4.5 is illustrated. It is evident that the increase of LCC in this scenario is higher compared to scenario 1-1.9. The reason for this difference is that scenario 2-4.5 has a larger hazard rate variation. As a result, the impact of climate

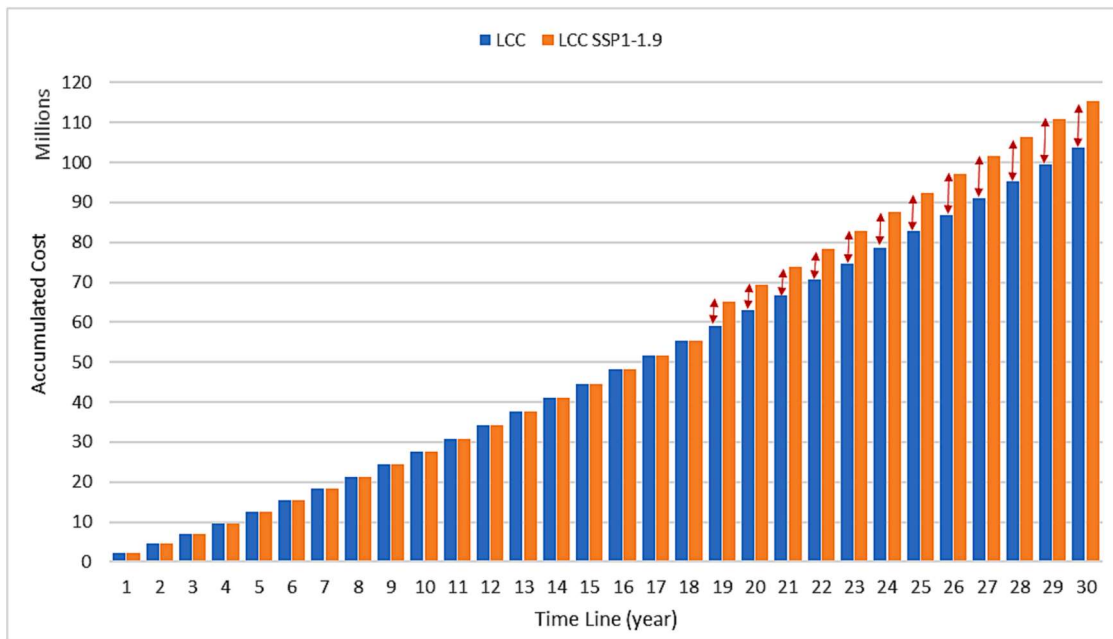


Fig. 22. Estimation of LCC under scenario1-1.9.

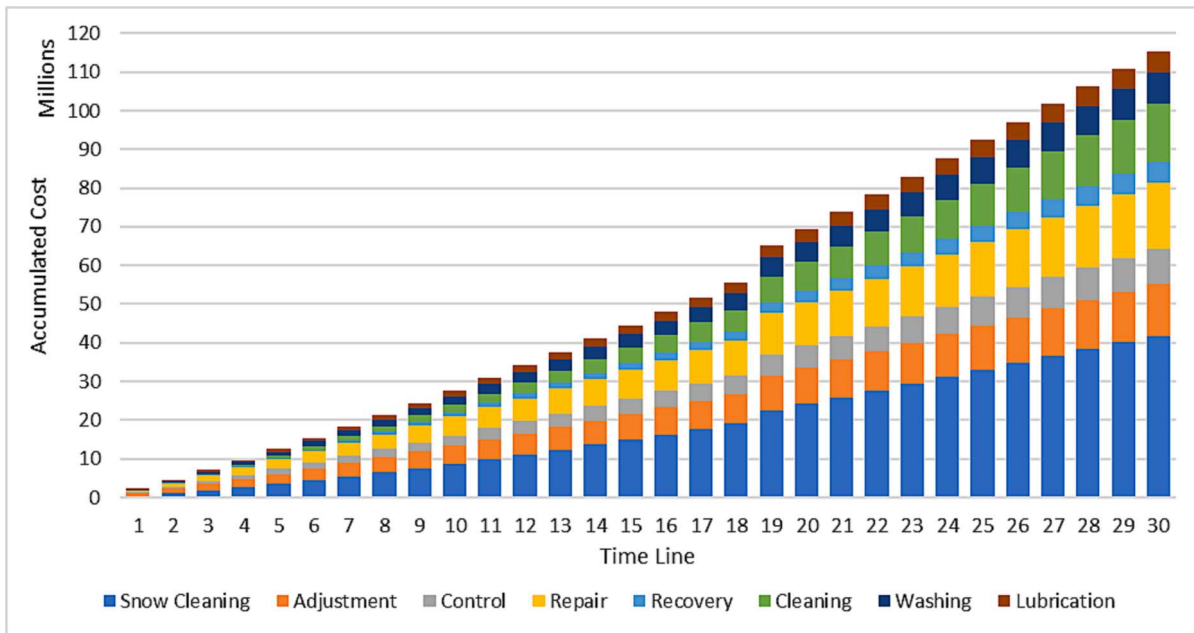


Fig. 23. Action-based estimation of LCC under scenario 1–1.9.

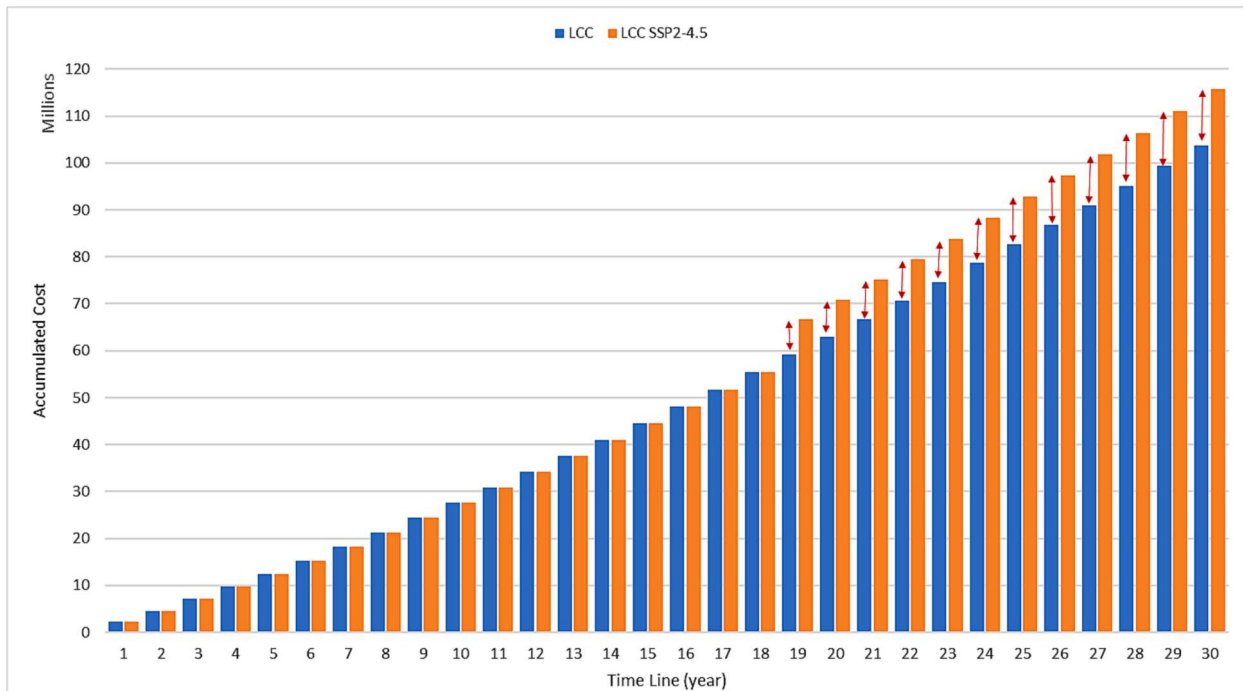


Fig. 24. Estimation of LCC under scenario2-4.5.

change parameters on the LCC has more effect in SSP 2–4.5, leading to a greater variation in costs over the specified period. Fig. 25 represents the estimation of LCC under SSP1-2.6, SSP3-7, and SSP5-8 scenarios. In all SSP scenarios, the LCC will increase when the impact of weather parameters is considered. The analyses show that SPP2-4.5 and SSP3-7 reveal the highest increment, almost 11.6 percent.

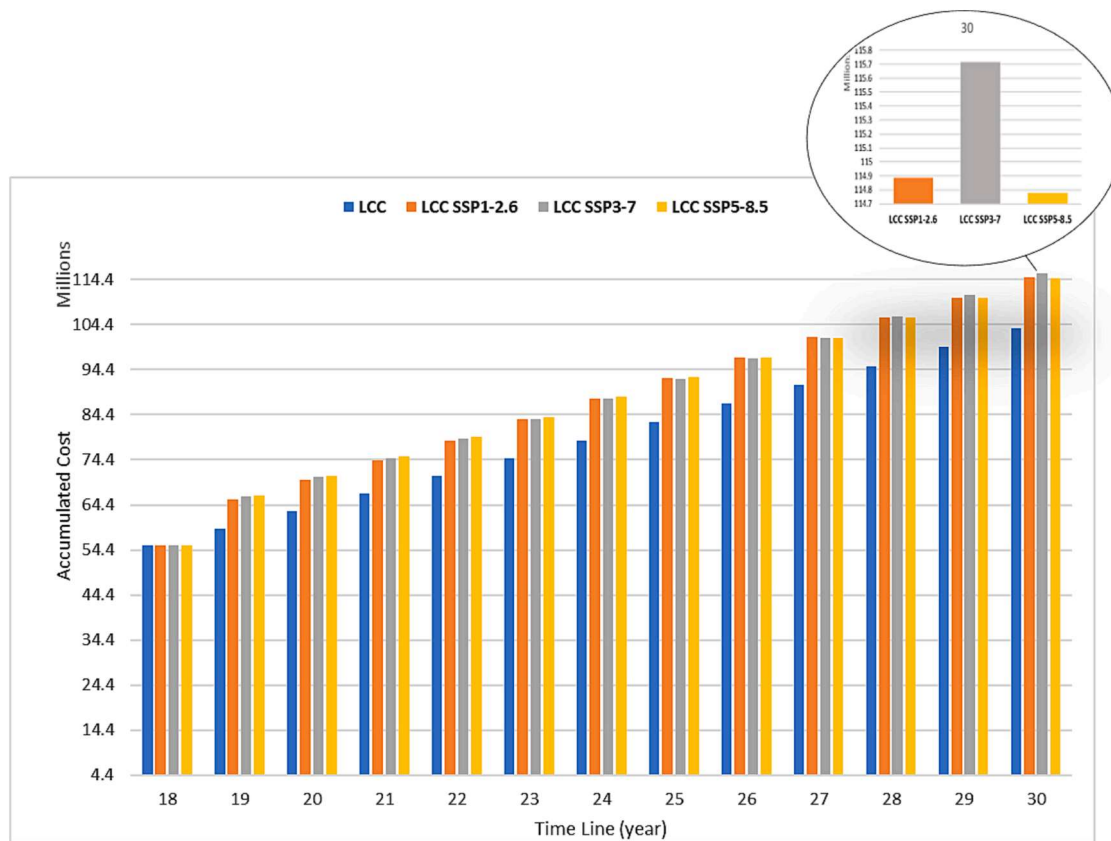


Fig. 25. Estimation of LCC for other scenarios.

## 5. Discussion and results

Comprehensive reliability analyses have been performed on the number of S&C assets installed in the North region of Sweden, considering homogeneity and heterogeneity factors. The previous research (Calle-Cordón, Á et al., (2017); Calle-Cordón, A. et al.,

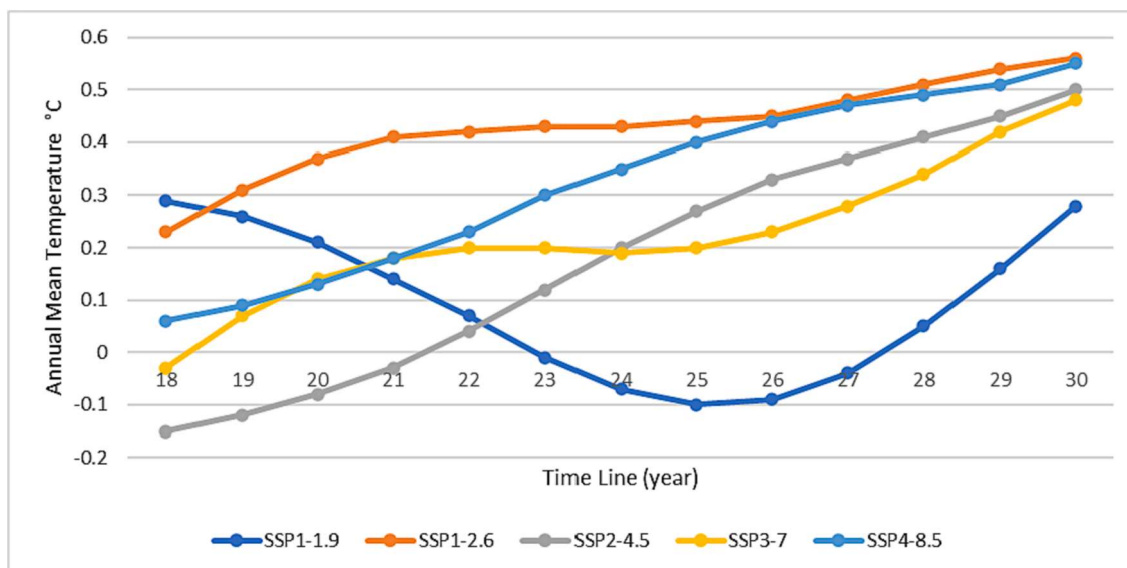


Fig. 26. The variation of annual mean temperature according to SSPs scenarios of the period 18–30.

(2018)) assumed that the failure occurrence follows the same Weibull distribution for all S&Cs and actions while calculating MTBF in LCC formulation, whereas, in this study, we estimate the RAMS parameter based on the underlying process, HPP, RP, and NHPP as shown in Table 6. In addition, LCC is broken down to perform maintenance actions associated with the component to explore the climate impacts on specific actions, resulting in updating maintenance actions and strategies.

The implications of SSPs scenarios on temperature, precipitation, and humidity are different; thus, the impact of SSPs on hazard rate will also be different. Our analyses show the combined impact of precipitation, humidity, and temperature on hazard rate under SSPs scenarios has a positive effect, i.e.  $\gamma_k \geq 0$ . In this case, LCC under SSP scenarios is greater than LCC without climate impact.

The impact of SSPs scenarios on temperature is shown in Fig. 26 from years 18 to 30. This figure shows that the annual mean temperature under different scenarios may increase (scenario SSP1-2.6) or decrease (scenario SSP1-1.9) from year 18 till year 26. The temperature has inverse effects on hazard rate according to Cox PH analysis. If we consider only the temperature covariate, it can have a negative impact ( $\gamma_k \leq 0$ ) on the hazard rate under scenario SSP1-1.9. Note that precipitation has a direct effect on hazard rate with a high ratio, while temperature and humidity have inverse effects according to Cox PH analysis; therefore, the combined impact of these weather parameters on hazard rate has a positive impact (see Table 7).

Corresponding to each SSPs scenarios, we can define LCC scenarios i.e. LCC1-1.9, LCC1.2.6, LCC2-4.5, LCC3-7, and LCC5-8.5. All the LCC scenarios are close to each other due to combined hazard rate variation, which is close to each other (see Fig. 27). These differences for LCC1-1.9, LCC1.2.6, LCC2-4.5, LCC3-7, and LCC5-8.5 are 11.2 %, 10.8 %, 11.6 %, 11.6 %, and 10.7 % respectively. It may be noted that the difference between ordinary LCC and LCC under SSPs scenarios is notable. SMHI predicted that snow precipitation will reduce and it is expected to experience a reduction trend in winter maintenance cost based on RCP scenarios; however, the impact of zero crossing will increase in the future. Therefore, the frequency of ice removal (snow cleaning) activity will increase in the future.

It may be noted that various uncertainty sources affect LCC estimation, including (I) uncertainty in RAMS parameters due to their probabilistic nature and (II) uncertainty associated with monetary and cost parameters. One can perform sensitivity analyses and identify the sensitive parameters that affect the research outcome.

The outcome of this research can help decision-makers plan the budget according to the considered scenario or design the needed activities for climate change adaptation. All calculations in this study are without considering the climate change adaptation activity and its impacts on hazard rate and associated maintenance strategies.

## 6. Conclusion

This paper presents a methodological framework to assess the impact of climate change on the LCC of switches and crossing in the North region of Sweden. The LCC analysis is a helpful tool for infrastructure managers to compare different intervention strategies and select the most desirable option based on the RAMS parameters.

Railway infrastructure is expected to be more susceptible to natural disasters and will continue to face increased climate-related risks. However, it is important to integrate various climate projection trajectories with a high level of spatial precision with RAMS parameters across various stressors and perform cost/benefit trade-offs across a range of adaptation measures.

Recent research shows that the effect of climate change on transport infrastructures' operation is noticeable. Therefore, decision-makers need to consider climate change consequences in their decision-making process. This paper proposes the new LCC methodology, considering climate-related incidents and future climate projections. We have faced several challenges, including data quality

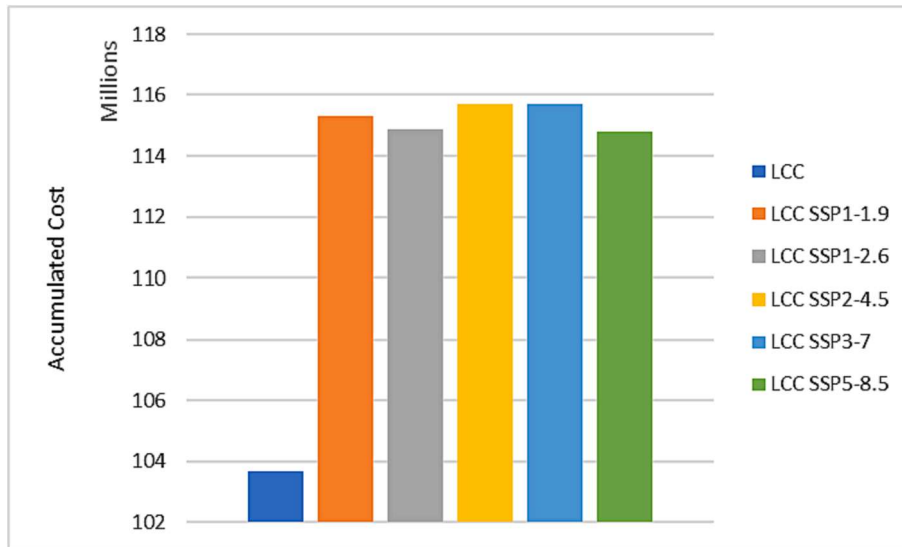


Fig. 27. LCC without SSPs scenarios and LCC with SSPs scenarios of the 30th year.

and silos data sources. In our use-case, the existing databases are not designed to capture all the climatic impacts and there is a need to upgrade the railway infrastructure data collection system. In addition, there is a need to utilize more IoT and sensor technology at stations to collect more accurate weather parameters. The long-distance of weather stations has a significant impact on the identification of underlying failure causes.

Comprehensive LCC assessment requires considering various parameters (technical and monetary) in the model structure. This study focuses more on corrective maintenance actions due to the stochastic nature of the failure events and relaxes other potential costs, including acquisition costs, preventive actions, and phase-out costs.

This study represents how maintenance cost and associated actions under various climate parameters are changing, which provide insight for infrastructure manager for better seasonal operation and maintenance planning and select the most critical climate adaptation measure that poses higher cost on infrastructure operation and maintenance over the years.

The results have shown that precipitation, temperature, and humidity are significant weather factors in selected use case. Furthermore, our analyses show that LCC under SSP's scenario experiences higher costs, about 11 %, than LCC without considering climate impacts. This means following the current maintenance planning resulted in more corrective actions and required implementation of climate adaptation actions and preventive measures to cope with adverse climatic consequences.

In the future, we will utilize machine learning tools to improve data quality and identify the correlation between covariates and failure incidents. In addition, there is a need for a more rigorous investigation of climate-related stressors beyond temperature, precipitation, and humidity, including vegetation fire, groundwater level, and extreme climate events.

### CRedit authorship contribution statement

**Khosro Soleimani-Chamkhorami:** Conceptualization, Data curation, Formal analysis, Investigation, Methodology, Software, Validation, Visualization, Writing – original draft, Writing – review & editing. **A.H.S Garmabaki:** Conceptualization, Data curation, Funding acquisition, Investigation, Methodology, Project administration, Supervision, Writing – original draft, Writing – review & editing. **Ahmad Kasraei:** Conceptualization, Data curation, Formal analysis, Methodology, Software, Validation, Writing – original draft, Writing – review & editing. **Stephen M. Famurewa:** Formal analysis, Methodology, Writing – original draft. **Johan Odelius:** Data curation, Formal analysis, Software, Writing – original draft. **Gustav Strandberg:** Data curation, Visualization, Writing – original draft.

### Declaration of competing interest

The authors declare that they have no known competing financial interests or personal relationships that could have appeared to influence the work reported in this paper.

### Data availability

The censored data are available on the request due to confidential agreement.

### Acknowledgments

Authors gratefully acknowledge the funding provided by Sweden's innovation agency, Vinnova, to the project titled "Adapting Urban Rail Infrastructure to Climate Change (AdaptUrbanRail)" (Grant no. 2021-02456) and "Robust infrastructure – Adapting railway maintenance to climate change (CliMaint)" (Grant no. 2019-03181)"; and Kempe foundation which providing Postdoctoral scholarship through (Grant no. JCK-3123). The authors gratefully acknowledge the in-kind support and collaboration of Trafikverket, SMHI, WSP AB, InfraNord, and Luleå Railway Research Center (JVTC).

### References

- Banar, M., Özdemir, A., 2015. An evaluation of railway passenger transport in Turkey using life cycle assessment and life cycle cost methods. *Transp. Res. Part D: Transp. Environ.* 41, 88–105.
- Barabadi, A., Barabady, J., Markeset, T., 2014. Application of reliability models with covariates in spare part prediction and optimization—a case study. *Reliab. Eng. Syst. Saf.* 123, 1–7.
- Bendell, A., Wightman, D.W., Walker, E.V., 1991. Applying proportional hazards modelling in reliability. *Reliab. Eng. Syst. Saf.* 34 (1), 35–53.
- Blackwood, L., Renaud, F.G., 2022. Barriers and tools for implementing Nature-based solutions for rail climate change adaptation. *Transp. Res. Part D: Transp. Environ.* 113.
- Cahyo, W.N., Raben, R.S.I., Prawahandaru, H., Swasono, B.A., Sutartono, R.T., Immawan, T., 2021. Policy Analysis on Spare Part Inventory of Critical Asset with Life Cycle Cost Approach. *J. Phys. Conf. Ser.* 1764 (1).
- Calle-Cordón, Á., Jiménez-Redondo, N., Morales-Gámiz, F.J., García-Villena, F.A., Garmabaki, A.H.S., Odelius, J., 2017. Integration of RAMS in LCC analysis for linear transport infrastructures. A case study for railways. *IOP Conference Series: Materials Science and Engineering* 236, 012106.
- Calle-Cordón, A., Jiménez-Redondo, N., Morales-Gámiz, J., García-Villena, F., Peralta-Escalante, J., Garmabaki, A., Famurewa, S.M., Duarte, E., Morgado, J., 2018. Combined RAMS and LCC analysis in railway and road transport infrastructures. *Proceedings of the 7th Transport Research Arena TRA*.
- Chen, C., Liu, Y., Wang, S., Sun, X., Di Cairano-Gilfedder, C., Titmus, S., Syntetos, A.A., 2020. Predictive maintenance using cox proportional hazard deep learning. *Adv. Eng. Inf.* 44.
- Chinowsky, P., Helman, J., Gulati, S., Neumann, J., Martinich, J., 2019. Impacts of climate change on operation of the US rail network. *Transp. Policy* 75, 183–191.
- Cox, D.R., 1972. Regression models and life-tables. *J. Roy. Stat. Soc.: Ser. B (Methodol.)* 34 (2), 187–202.
- Ebeling, C.E., 2019. *An introduction to reliability and maintainability engineering*. Waveland Press.

- Galar, D., Sandborn, P., Kumar, U., 2017. Maintenance costs and life cycle cost analysis. CRC Press.
- Garmabaki, A., Kumar, U., 2019. Robust infrastructure – Adapting railway maintenance to climate change (ClimMaint). Luleå University of Technology, Vinnova.
- Garmabaki, A., Ahmadi, A., Block, J., Pham, H., Kumar, U., 2016. A reliability decision framework for multiple repairable units. *Reliab. Eng. Syst. Saf.* 150, 78–88.
- Garmabaki, A., Thaduri, A., Famurewa, S., Kumar, U., 2021. Adapting railway maintenance to climate change. *Sustainability* 13 (24), 13856.
- Hamarat, M.Z., Kaewunruen, S., Papaefias, M., 2019. A Life-Cycle Cost Analysis of Railway Turnouts Exposed to Climate Uncertainties. *A Life-Cycle Cost Analysis of Railway Turnouts Exposed to Climate Uncertainties* 471.
- Kasraei, A., Garmabaki, A.H.S., Odelius, J., Famurewa, S.M., Chamkhorami, K.S., Strandberg, G., 2024. Climate change impacts assessment on railway infrastructure in urban environments. *Sustain. Cities Soc.* 101.
- Kumar, D., Klefsjö, B., 1994. Proportional hazards model: a review. *Reliab. Eng. Syst. Saf.* 44 (2), 177–188.
- Kumar, D., Klefsjö, B., Kumar, U., 1992. Reliability analysis of power transmission cables of electric mine loaders using the proportional hazards model. *Reliab. Eng. Syst. Saf.* 37 (3), 217–222.
- Liu, B., Liang, Z., Parlikad, A.K., Xie, M., Kuo, W., 2020. Condition-based maintenance for systems with aging and cumulative damage based on proportional hazards model. In: Crespo Márquez, A., Macchi, M., Parlikad, A.K. (Eds.), *Value Based and Intelligent Asset Management: Mastering the Asset Management Transformation in Industrial Plants and Infrastructures*. Springer International Publishing, Cham, pp. 211–231.
- Liu, K., Wang, M., Zhou, T., 2021. Increasing costs to Chinese railway infrastructure by extreme precipitation in a warmer world. *Transp. Res. Part D: Transp. Environ.* 93.
- Mazidi, P., Bertling Tjernberg, L., Sanz Bobi, M.A., 2017. Wind turbine prognostics and maintenance management based on a hybrid approach of neural networks and a proportional hazards model. *Proc. Inst. Mech. Eng. Part C: J. Risk Reliab.* 231 (2), 121–129.
- Meteoblue (2023) History and climate, climate change.** Available at: <https://www.meteoblue.com>.
- Mishra, M., Odelius, J., Thaduri, A., Nissen, A., Rantatalo, M., 2017. Particle filter-based prognostic approach for railway track geometry. *Mech. Syst. Sig. Process.* 96, 226–238.
- Mitoulis, S.-A., Bompa, D.V., Argyroudis, S., 2023. Sustainability and climate resilience metrics and trade-offs in transport infrastructure asset recovery. *Transp. Res. Part D: Transp. Environ.* 121.
- Neumann, J.E., Chinowsky, P., Helman, J., Black, M., Fant, C., Strzepek, K., Martinich, J., 2021. Climate effects on US infrastructure: the economics of adaptation for rail, roads, and coastal development. *Clim. Change* 167 (3–4), 44.
- Nissen, A., 2009. Development of life cycle cost model and analyses for railway switches and crossings. *Int. J. COMADEM* 12 (2), 10–19.
- O'Neill, B.C., Kriegler, E., Riahi, K., Ebi, K.L., Hallegatte, S., Carter, T.R., Mathur, R., van Vuuren, D.P., 2014. A new scenario framework for climate change research: the concept of shared socioeconomic pathways. *Clim. Change* 122 (3), 387–400.
- Palin, E.J., Stipanovic Oslakovic, I., Gavin, K., Quinn, A., 2021. Implications of climate change for railway infrastructure. *Wiley Interdiscip. Rev. Clim. Chang.* 12 (5), e728.
- Pirayonesi, S.M., El-Diraby, T., 2021. Climate change impact on infrastructure: A machine learning solution for predicting pavement condition index. *Constr. Build. Mater.* 306.
- Pu, H., Cai, L., Song, T., Schonfeld, P., Hu, J., 2023. Minimizing costs and carbon emissions in railway alignment optimization: A bi-objective model. *Transp. Res. Part D: Transp. Environ.* 116, 103615.
- Qiao, Y., Guo, Y., Stoner, A.M.K., Santos, J., 2022. Impacts of future climate change on flexible road pavement economics: A life cycle costs analysis of 24 case studies across the United States. *Sustain. Cities Soc.* 80.
- SMHI (2023) Advanced Climate Change Scenario Service.** Available at: <https://www.smhi.se/en/climate/future-climate/advanced-climate-change-scenario-service/met/sverige/medelnederbord/rcp85/2011-2040/year/abs>.
- Swarna, S.T., Hossain, K., Bernier, A., 2022. Climate change adaptation strategies for Canadian asphalt pavements; Part 2: Life cycle assessment and life cycle cost analysis. *J. Clean. Prod.* 370.
- Thaduri, A., Garmabaki, A., Kumar, U., 2021. Impact of climate change on railway operation and maintenance in Sweden: A State-of-the-art review. *Maintenance, Reliability and Condition Monitoring (MRCM)* 1 (2), 52–70.
- Thijssens, O.W.M., Verhagen, W.J.C., 2020. Application of extended cox regression model to time-on-wing data of aircraft repairables. *Reliab. Eng. Syst. Saf.* 204.
- Wang, T., Qu, Z., Yang, Z., Nichol, T., Clarke, G., Ge, Y., 2020. Climate change research on transportation systems: Climate risks, adaptation and planning. *Transp. Res. Part D: Transp. Environ.* 88, 102553.
- World Bank Group (2021) Climate Change Knowledge Portal.** Available at: <https://climateknowledgeportal.worldbank.org/>.
- Zheng, H., Kong, X., Xu, H., Yang, J., 2021. Reliability analysis of products based on proportional hazard model with degradation trend and environmental factor. *Reliab. Eng. Syst. Saf.* 216.
- Zheng, R., Wang, J., Zhang, Y., 2023. A hybrid repair-replacement policy in the proportional hazards model. *Eur. J. Oper. Res.* 304 (3), 1011–1021.